DEFORMATIONS IN A SOIL UNDER DYNAMIC LOADING

THE DETERMINATION AND ANALYSIS OF DEFORMATIONS IN A SOIL UNDER DYNAMIC LOADING

by

Henry R. Krzywicki, B.A.Sc.
(University of Waterloo)

A Thesis
Submitted to the Faculty of Graduate Studies
in Partial Fulfilment of the Requirements
for the Degree
Master of Engineering

McMaster University
September, 1964

MASTER OF ENGINEERING
(Civil Engineering)

McMASTER UNIVERSITY
Hamilton, Ontario

TITLE: The Determination and Analysis of Deformations in A Soil under Dynamic Loading.

AUTHOR: Henry R. Krzywicki, B.A.Sc. (University of Waterloo).

SUPERVISOR: Professor N.E. Wilson, Department of Civil Engineering.

NUMBER OF PAGES: viii, 94

SCOPE AND CONTENTS:

This Thesis describes a method for determining and analysing the deformations in peat caused by a driven rigid wheel. Markers were placed in the peat sample and radiographs were taken as the wheel travelled over the surface of the peat. An analysis of the data revealed that a unique relationship existed between the positions of the markers and the positions of the wheel. The paths of the principal stress trajectories were determined by a graphical method; from the principal stress trajectories, it was possible to find the surfaces of maximum shear.

The purpose of determining these surfaces is to allow the equilibrium of the soil mass to be investigated by the present theories in soil mechanics; it is to draw an analogy to the analysis of slope stability problems.

ACKNOWLEDGEMENTS

I should like to acknowledge my debt to Professor N.E. Wilson initially for his advice during the course of the research work and finally for the optomistic attitude he displayed during periods of crisis.

The research for this paper was supported (in part) by the Defence Research Board of Canada, Grant Number 9768-04.

TABLE OF CONTENTS

LIST OF ILLUSTRATIONS

FIGURE PAGE

SUMMARY

A fundamental approach to the problem of vehicle mobility, by the study of deformations and stresses of the soil as a vehicle moves, is described in this thesis.

A driven rigid wheel was constructed to run over a sample of amorphous granular peat. Metal markers were placed throughout the peat and a record of their movements was obtained as the wheel travelled over the peat. The movements of the markers were recorded on films by using an X-ray technique.

The markers moved in cardioid paths as the wheel travelled. The marker movement for any location within the sample was obtained from the unique relationships which existed between the positions of the wheel and the movements of the markers.

The trajectories of the principal stresses were determined by a graphical method. Using an assumption regarding the angle of internal friction for amorphous granular peat, the surfaces of maximum shear were obtained.

The surfaces of maximum shear resembled the configurations normally associated with slope stability problems

in soil mechanics.

The similarity between the maximum shear surface configurations led to the conclusion that the problems associated with mechanics of mobility may be approached with methods available in soil mechanics. The equilibrium of soil under a moving wheel appears analogous to slope stability. If the surfaces of maximum shear and the shear stresses are known, slope stability problems may be analysed.

CHAPTER I

INTRODUCTION

Until recently, research conducted on vehicle design and mobility has dealt with the function of the vehicle as a whole or with that portion which comes into contact with the supporting mass. Tests have been established which can evaluate the performance of the vehicle; the work of Thomson is a typical example (Thomson, 1958; 1960; 1961).

Some workers in this field are of the opinion that a more basic approach to the problem of vehicle design in terms of mobility is necessary. As the terrain over which a vehicle traverses is the basic obstruction to the vehicle, a fundmental approach to the problem of mobility is the study of deformations and stresses of the terrain as a vehicle moves.

This thesis approaches the problem of vehicle mobility at a fundamental level. The deformations which were induced by a driven rigid wheel were measured using an x-ray technique.

A test bin filled with peat was exposed to the load of a driven rigid wheel. As the wheel passed over the peat, radiographs were taken of metal markers which had been placed

throughout the peat. An analysis of the radiographs revealed that the markers, and presumably the peat which surrounds them, move in paths which resemble cardioids (heart-shaped). The upper markers followed cardioid paths which were much larger in size than lower markers. Relationships were found between the marker movements and the positions of the wheel.

By using a method developed by Haefeli, the trajectories of the principal stresses were found (Haefeli, 1944). This information, coupled with the knowledge that the markers moved in cardioid paths, permitted an analysis of the movement. Three distinct causes of movement were detected. The first movement was attributed to direct wave action which preceeded the wheel. The rotational effect of the wheel created the movement which followed the wave action; the generation and dissipation of a wave behind the wheel accounted for the final movement.

This work, which is presented as a fundamental approach to the problem of vehicle mobility, serves as a stepping stone for further research projects. The final goal is a thorough understanding of the soil movement due to the action of a vehicle.

CHAPTER II

LITERATURE REVIEW

In general, the relationship which exists between engineering and muskeg research can be divided into four catagories, namely, classification, engineering properties, construction techniques and vehicle mobility.

(a) Classification

The basic problem of muskeg classification has been thoroughly investigated by Radforth (Radforth, 1952; 1957). An engineering classification system has been established using a letter code describing vegetal cover which can be related to the underlying peat.

(b) Engineering Properties

Many investigators were interested in the engineering properties of peat (Hanrahan, 1954). Schroeder and Wilson were concerned with the consolidation characteristics of peat from the viewpoint of primary and secondary consolidation (Schroeder and Wilson, 1962). They showed that the rate of drainage governed the primary consolidation while the viscous characteristics governed the secondary consolidation. Adams performed triaxial compression tests on peat and he concluded that the consolidation of peat was mainly the expulsion of pore water under excess hydrostatic pressure (Adams, 1961).

The shear strength of peat has been investigated by MacFarlane and Rutka by means of a field vane (MacFarlane and Rutka, 1962). They found that there was no evident correlation of vane shear strength with muskeg type. Anderson, on the other hand, after conducting some research with a field vane concluded that general ranges of shear strength could be predicted on the basis of surface vegetal cover or the Radforth classification (Anderson, 1962).

The measurement of viscosity to evaluate the engineering properties of soils is a new and interesting approach. As viscosity is a function of shear rate, the effect of shear rate on shear strength can be observed. Eden and Kubota were able to measure the viscosity of Leda clay and compare their results to the shear strength obtained using other methods (Eden and Kubota, 1962). Krzywicki and Wilson attempted to measure the viscosity of amorphous granular peat (Krzywicki and Wilson, 1964). Their study indicated that viscosity measurements could provide helpful data for use in the field of vehicle mobility.

(c) Construction Techniques

Field experience, leading to the development of new techniques in construction over organic terrain, is an important topic in muskeg research. In this area, the theories which are derived from laboratory tests on the engineering

properties of peat can be tested. Long term records by Ripley and Leonoff on the settlement of an embankment provided data to substantiate laboratory test results on consolidation (Ripley and Leonoff, 1961). The construction of roads over organic terrain is a major problem in development operations. Brawner discussed various methods of excavation and displacement as well as the use of sand drains to accelerate consolidation (Brawner, 1958). The technique of using deep drainage ditches and toe-shorting ahead of embankment placing was described by Monaghan (Monaghan, 1963). Markowsky and Adams discussed the technique of anchoring transmission towers in shallow peat deposit (Markowsky and Adams, 1960).

(d) Vehicle Mobility

The problems associated with construction on organic terrain are not necessarily due to consolidation; the problems of access over organic terrain are greater than the problems associated with static loads. It is for this reason that a great deal of effort is being paid to vehicle mobility.

Until recently, research conducted on vehicle design and mobility has dealt with the function of the vehicle as a whole or with that portion which comes into contact with the supporting mass. Thomson performed full scale tests on various vehicles and suggested that a draw-bar coefficient (draw-bar pull ÷ gross vehicle weight) could be used as a measure of performance (Thomson, 1958). He established that

the significantdesign features affecting mobility performance were the location of the dynamic centre of gravity, belly width, track contact pressure and grouser spacing (Thomson, 1960). In addition, Thomson stated that the design of the vehicle should be based on the role which it would be expected to play in terms of mobility and function; then the range of conditions in which the vehicle is to operate should be established (Thomson, 1961).

The use of test rigs to determine the performance of wheels and tracks is very popular. Reece and Wills have experimented with a field unit on which the slip is controlled and the tractive effort and torque input are the measured values (Reece and Wills, 1961). McKibben and Davidson determined the relationship between the outside diameters of pneumatic implement tyres and their rolling resistances for given inflation pressures and field conditions (McKibben and Davidson, 1940).

Another approach to vehicle mobility has been the correlation of vehicle performance with soil parameters. The soil parameters were obtained from the relationship between sinkage and load. This approach has been used extensively by Bekker in his studies on vehicle mobility (Bekker, 1956; 1960; 1961). Goodman and Lee have adapted this approach to study the effects of remoulding the soil on vehicle mobility (Goodman

and Lee, 1961). Dickson measured simultaneously, with a tilting plate penetrometer, the vertical and horizontal soil reactions for a given sinkage and horizontal slippage (Dickson, 1962). In this manner, he showed a correlation between a vehicle and penetrometer behaviour.

As pressure sensing devices have become more compact and reliable, their use in vehicle mobility studies have increased. Vanden Berg used pressure cells developed by Cooper to record the soil pressure distribution under farm implement traffic (Vanden Berg et al., 1957; Cooper et al., 1957). By using this equipment, the investigators plotted a soil pressure distribution within the soil. Trabbic used a similar type of pressure cell, embedden in the tyre, to record the pressure on the tyre at the interface of the tyre and the soil (Trabbic et al.,1959). Strain gauges mounted on a wheel were used by Uffelman to obtain radial and tangential stress measurements (Uffelman, 1960).

The U.S. Army Corps of Engineers at the Waterways Experiment Station have been active in using pressure cells to measure pressures within the soil caused by full scale vehicles and by test rigs which utilize full scale components. Freitag and Knight used a commercially available pressure cell to measure the stresses in a yielding soil (Freitag and Knight, 1961). Freitag and Green used the same type of cell

to determine the distribution of stresses on an unyielding surface beneath a pneumatic tyre (Freitag and Green, 1961). Green, using a pressure cell developed by the Waterways Experiment Station, measured the pressures beneath prototype vehicles (Green, 1962). It should be emphasized that although some success has been achieved in measuring pressures within the soil, there exists a degree of uncertainty in the results.

The testing of full scale vehicles has not always been feasible or desirable. It was shown by Nuttall that a well developed scale model procedure is often desired for the following reasons: economy, precision in measurment, control of conditions, speed in developing data, adaptability and flexability of test facilites (Nuttall, 1949).

While progress has been made in the development of pressure cells to measure the pressures both in the soil and on the vehicle, very little effort has been made to examine the deformations in the soil which are caused by these pressures. McKibben observed the motion of soil particles under a rigid transport wheel (McKibben, 1938). He observed the movements by placing BB shot against the glass wall of a soil container (Fig. 1). More recently, Roscoe used x-ray methods to determine incremental strains throughout a soil mass (Roscoe, 1963). Although his study is not concerned with vehicle mobility, his work gave rise to the concept of using x-ray

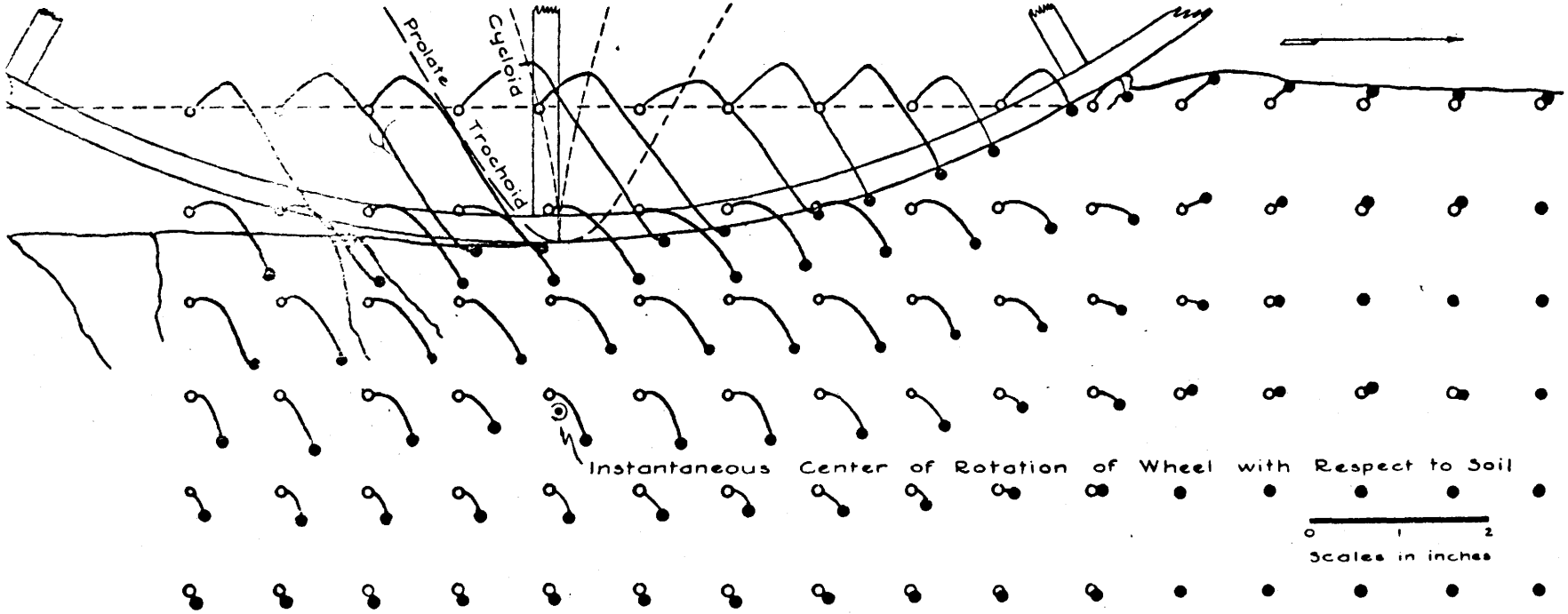

Motions of soil particles under a rigid transport wheel. (Note the cracks at the bottom of the wheel track, the location of the instantaneous center of rotation and the similarity between the prolate trochoid and the curves generated by the soil particles.)

FIG. 1 AFTER McKIBBEN (1938)

methods to determine the deformations in peat caused by a driven rigid wheel.

(e) The Analysis of Deformations in Soil

Assuming that the deformations are obtainable, a more intricate problem is the analysis of these deformations. A method of determining the principal stress trajectories from deformations was given by Haefeli (Haefeli, 1944). Haefeli's method offers a graphical solution for the principal stress trajectories by analysing the plastic or elastic deformations of a regular line network. This method was derived by using the fundamental concepts of soil and snow mechanics.

Methods, based on the fundamental theories of strain, offer an alternate approach to the analysis of deformations. Meyer described a method of determining the directions of principal strains by an analysis of elongations (Meyer, 1963). The directions of the principal strains are coincident with the directions of the principal stresses for an isotropic material. The assumption of isotropy permits the determination of the principal stress directions.

The method given by Meyer for analysing elongations and finite strains was not used, as the conditions were not satisfied. One condition was the exclusion of strain-free rotation from the measurements of strains. In addition,

the usual definition of strain was not applicable for incremental wheel travel, therefore, the values for the strains were unknown.

The determination of maximum shear surfaces from principal stress trajectories permits the problems associated with mechanics of mobility to be approached with the methods available in soil mechanics. The method given by Haefeli was used to determine the principal stress trajectories, as this method analysed deformations rather than strains.

CHAPTER III

THE PHYSICAL PROPERTIES OF AMORPHOUS GRANULAR PEAT

The peat used in this research work has been classified as amorphous granular peat according to MacFarlane (MacFarlane, 1958). The amorphous granular peat was found in an area 11 miles north of Parry Sound, Ontario. A typical aerial view of the terrain in the Parry Sound area is shown in Fig. 2. The area from which samples were taken is designated as Area 1 by the McMaster University "Organic and Associated Terrain Research Unit". The vegetal cover is termed EFI according to the Radforth muskeg classification system (Radforth, 1952).

The site of the sampling was in an area in which a vehicle had previously become immobilized. The subsequent towing operation caused much of the vegetal cover to be removed, exposing the underlying amorphous granular peat. When the peat was sampled, it had previously been remoulded by the action of the vehicle. In this remoulded state the peat had a moisture content in excess of 700% of the dry weight.

In order to make the peat as uniform as possible, the entire sample was passed through a #4 sieve (U.S. Standard). By this operation, the coarser fibrous material, which had

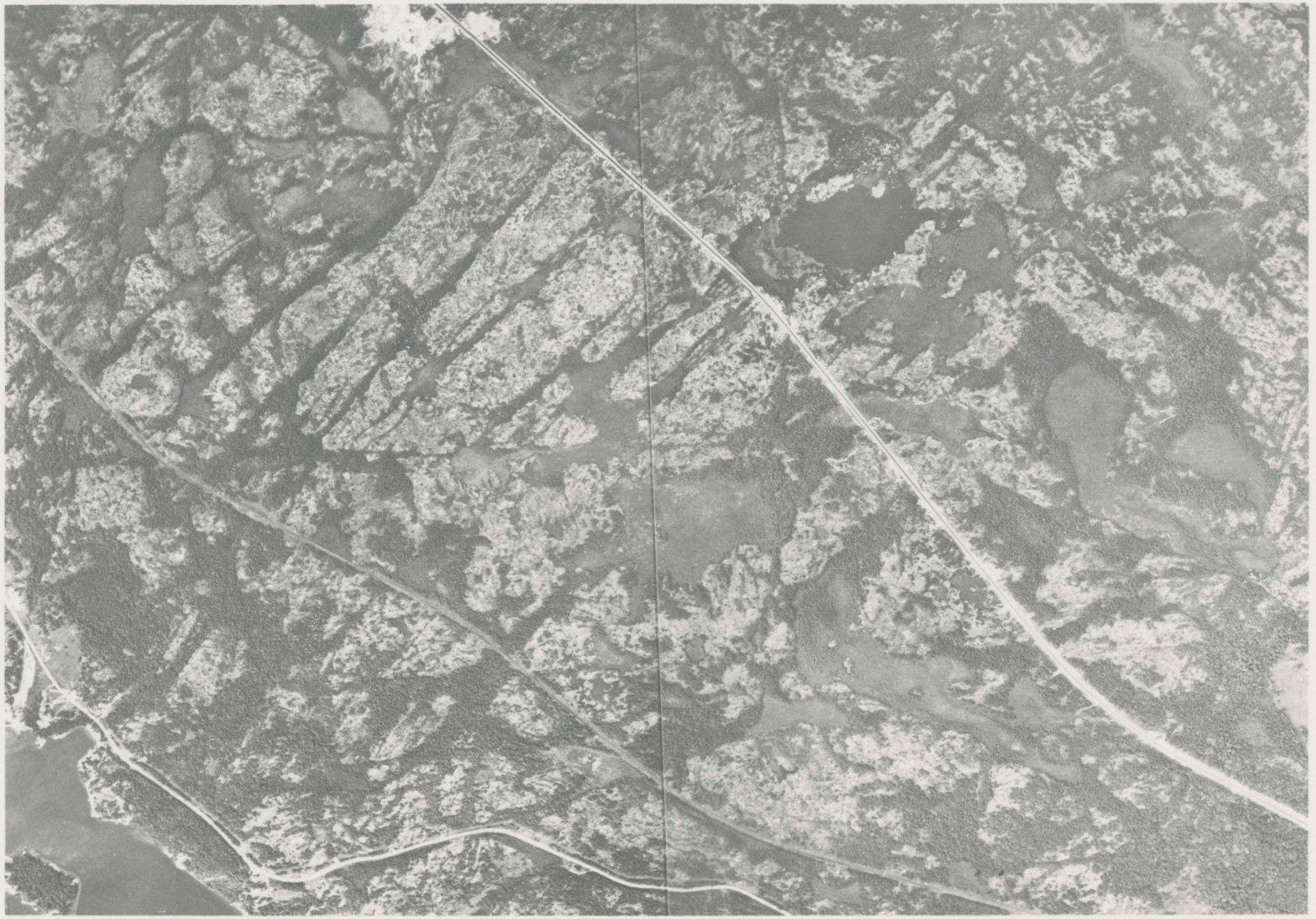

Fig. 2 Aerial View of Terrain in Parry Sound Area

become incorporated in the peat during the remoulding operation, was removed. Subsequent sieving removed very little fibrous material.

A trial run performed with the peat at the field moisture content showed that excessive sinkage occured and that the peat could not support the model load. Subsequently, the peat was air dried until the moisture content was reduced to a point where the modelload was satisfactorily supported by the peat; the moisture content was found to be approximately 660% of the dry weight. All moisture content determinations were conducted in an 85° C oven for a period of 24 hours.

The natural colour of the peat sample was dark brown to black and no apparent change in colour was observed after drying. The loss of weight upon ignition was found to be 70% of the oven dried weight of sample. The ignition loss tests were conducted in a 600° C muffle furnace for a period of one half hour.

In order to further classify this particular material, several tests, which are common in the field of soil mechanics, were performed. The liquid limit was found to be 565% and the plastic limit 247%; the flow curve for the Atterberg test is shown in Fig. 3. The specific gravity of the sample was calculated to be 1.4. A shear strength test was performed using a laboratory vane supplied by Wykeham Farrance Engineering

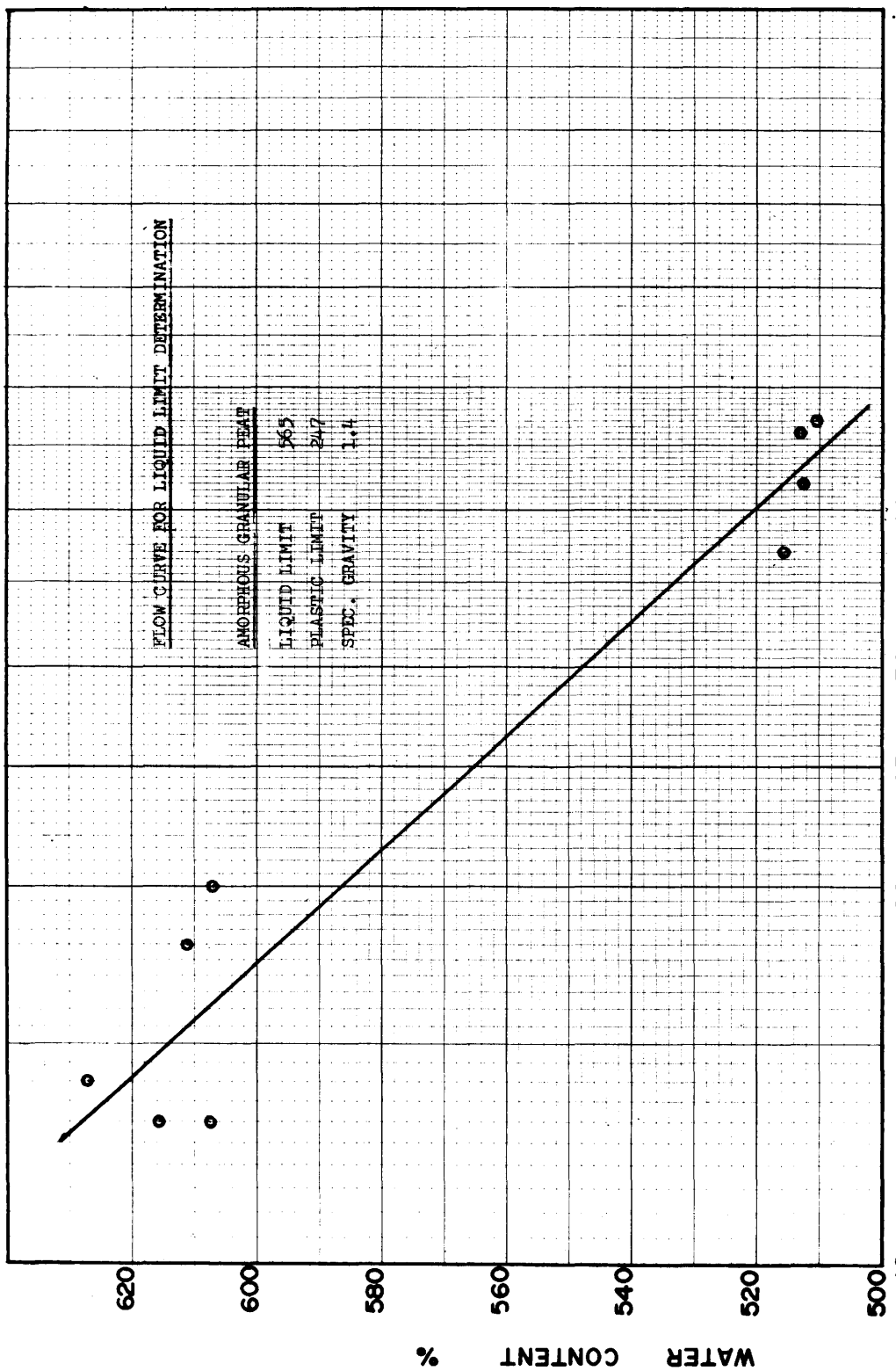

FIG. 3 FLOW CURVE

Limited. The vane has four thin rectangular blades which are welded to a shaft. When the vane is inserted into the sample and rotated the surface of failure can be approximated by a right circular cylinder having the diameter and height equal to that of the vane. In this case the vane was $\frac{1}{2}$ inch in diameter and $\frac{1}{2}$ inch high. The vane was connected to a Brookfield viscometer on which the speed of rotation could be varied. The Brookfield viscometer was used for the shear strength determination because the shear strength of the peat fell below the range of shear strengths which could be measured with the laboratory vane. The maximum torque applied to the peat sample was measured for various angular speeds and at various water contents. Torque readings were converted to shear strength by using the Cadling-Odenstad equation which is discussed in a work by Wilson (Wilson, 1963). At a moisture content of 660%, the shear strength was found to range between 0.06 and 0.08 pounds per square inch for angular velocities ranging from 3 to 60 degrees per second. (Fig. 4)

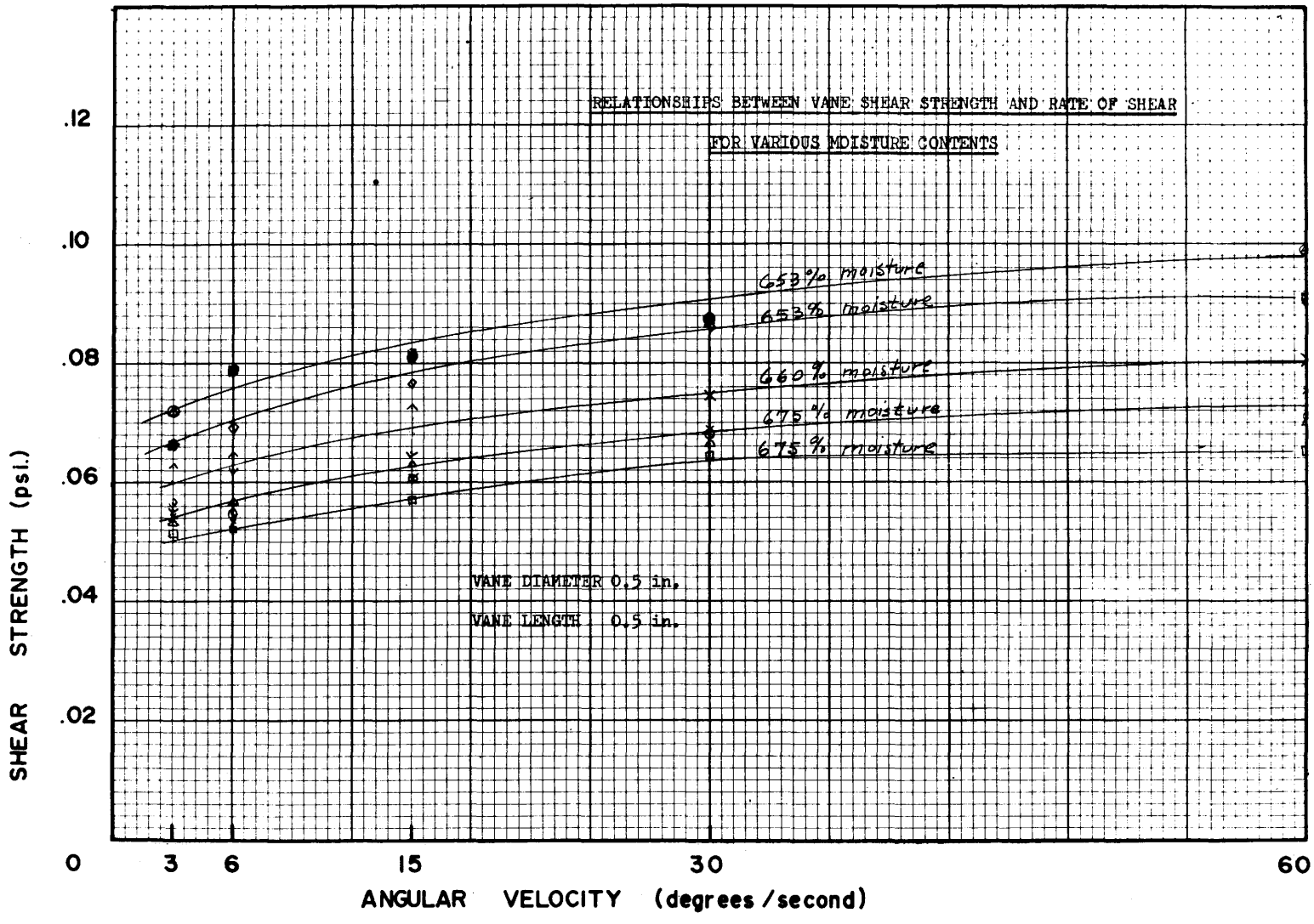

FIG. 4 SHEAR STRENGTH RELATIONSHIPS

CHAPTER IV

TEST APPARATUS

The object of this research work is to determine the deformations in peat which are caused by a driven rigid wheel (Fig. 5). A motorized rigid wheel was constructed so that it ran over a sample of amorphous granular peat. Metal markers were placed throughout the peat and a record of their movements was obtained as the wheel passed over the peat. The movement of the markers was recorded on film using an X-ray technique.

(a) Driven Rigid Wheel

During the test, the wheel was driven over the peat; the motor, with its associated carriage, was supported on an independent track. The wheel moved in a longitudinal direction and sank into the peat while the motor and carriage ran along the track. The wheel portion of the apparatus was constructed from a piece of aluminum tubing, 3 inches long, with an outside diameter of 6.65 inches and a wall thickness of 0.25 inches. Side plates through which the axle was located, were welded to the ends of the tubing. Fourteen lucite grousers (3" long x $\frac{1}{4}$" wide x 1/8" thick) were bonded around the periphery of the wheel to increase the tractive effort. Calculations of slip and sinkage were based on the

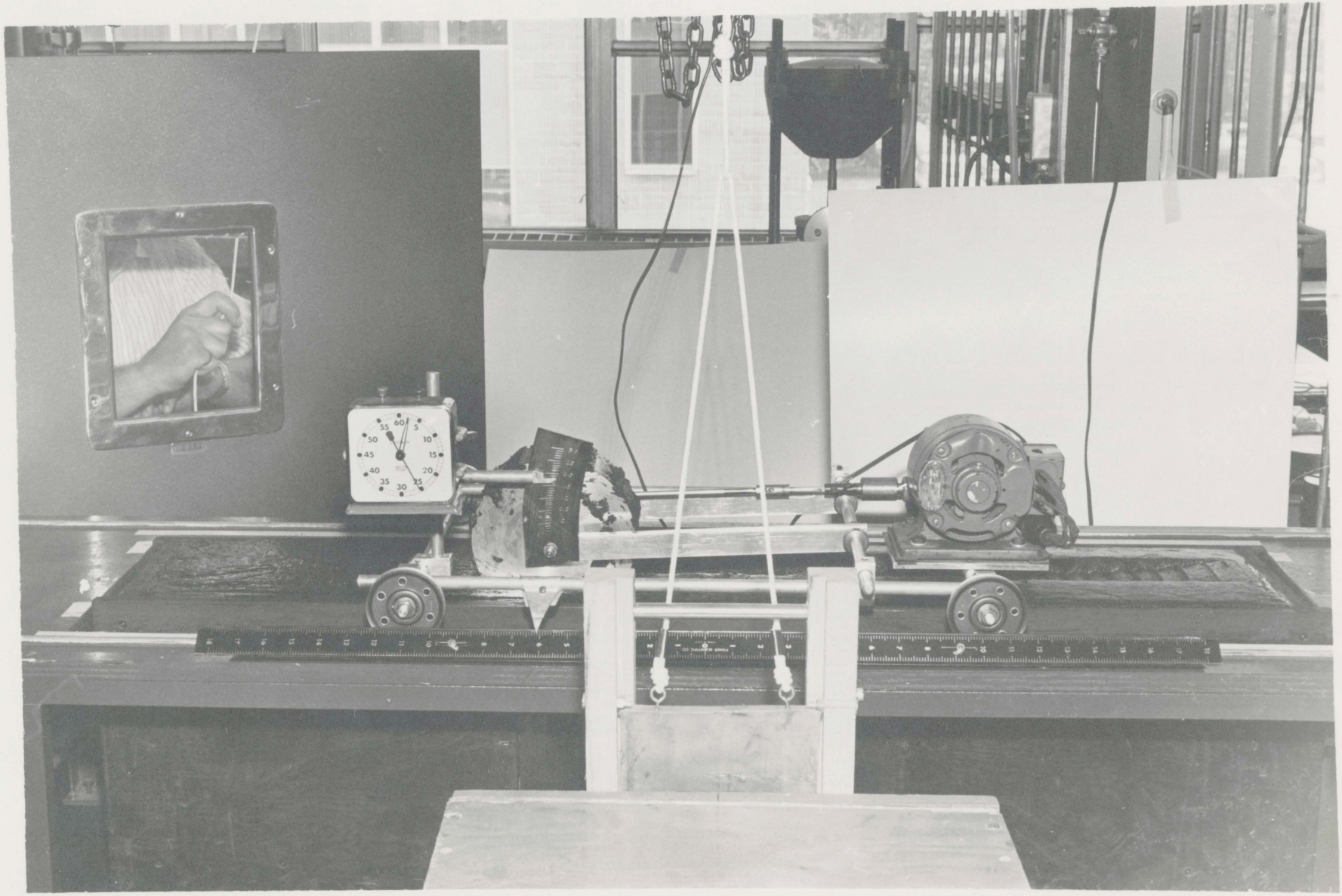

Fig. 5 Test Unit in Operation

outside diameter of the wheel; this was 6.9 inches which included an allowance for the lucite grousers. The suspended weight of the wheel assembly was 4.6 pounds.

Power was applied to the wheel by a 1/20 H.P. synchronous electric motor, which was equipped with a 43 to 1 reducing gear box. A further reduction in speed of 40 to 1 was obtained by a worm and worm gear located on the aluminum wheel. The wheel, after gear reduction, travelled at a rate of 0.403 inches per second at zero slip. The power was transmitted through a universal joint and adjustable drive shaft. With this system, the motor remained fixed to the carriage while the wheel assembly moved in the longitudinal direction and sank into the peat. The carriage which holds the motor and wheel assembly was constructed from $\frac{1}{2}$ inch aluminum rods clamped together. The four wheels which supported the carriage had ball bearings to minimize the power loss due to friction. Bearings were used wherever possible to minimize the unknown effects of friction. A photograph showing the carriage and drive assembly is shown in Fig. 6.

Indicators were positioned on the carriage to measure sinkage, time and position. A photograph of the unit in operation is shown in Fig. 5.

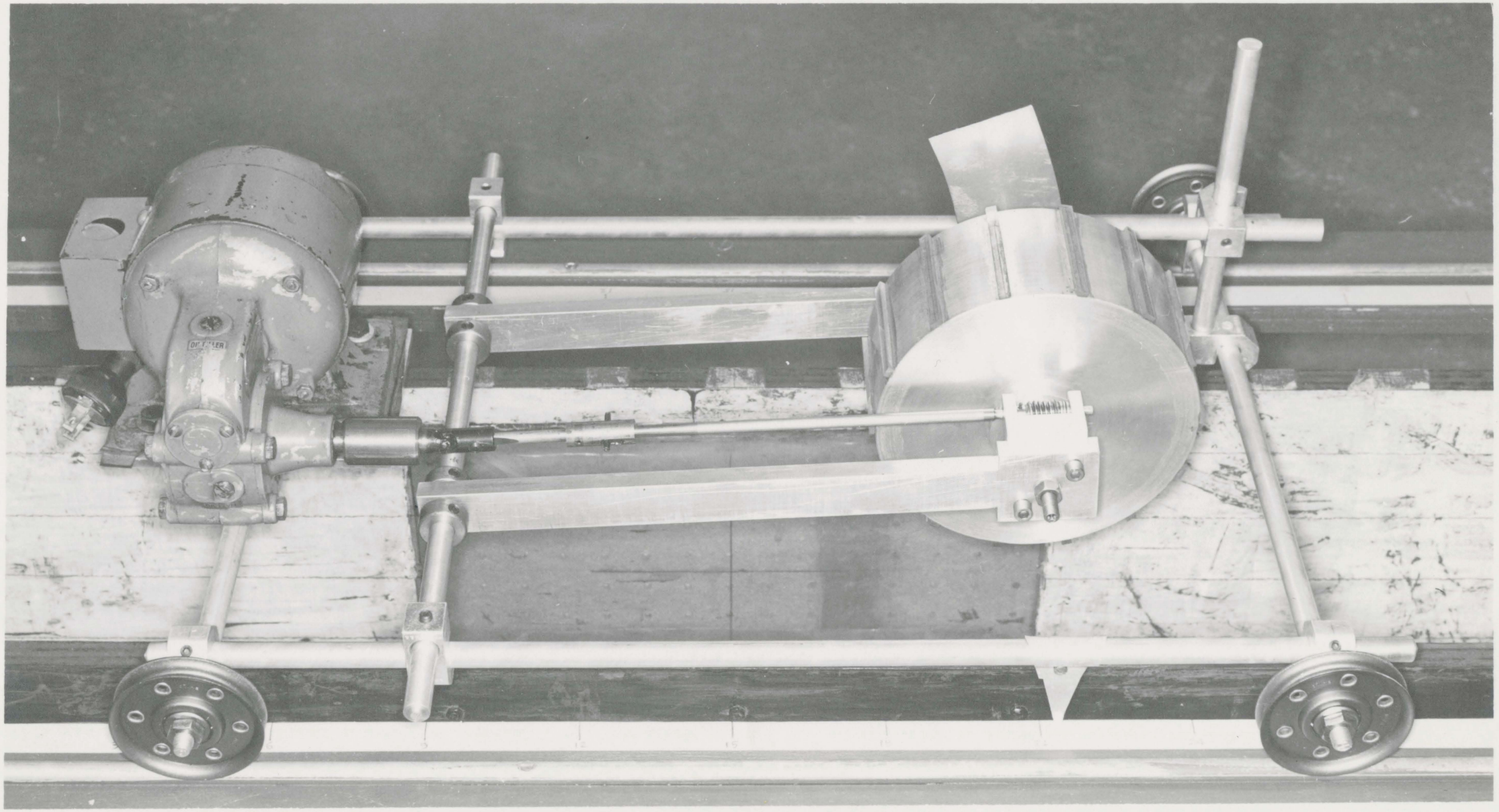

Fig. 6 Wheel Carriage and Drive Assembly

(b) Test Bin

The test bin was constructed from 3/4 inch plywood and the inside dimensions were 8 inches wide by 10½ inches deep by 45 inches long. Waterproofing was applied to the inside of the bin. Two lucite windows (8½" wide x 15" long x 1/8" thick) were located in the side walls at the centre of the bin. With the bin filled with peat, the gross weight was approximately 280 pounds. Two persons were able to lift the bin for positioning before the test and for disassembling the apparatus after the test.

(c) Track Unit

The track unit, which supported the wheel assembly, was constructed from a piece of 3/4 inch plywood resting on a metal frame (Fig. 7). Two aluminum rods (½" diameter) served as tracks on which the carriage travelled. Leveling screws were located on the feet of the unit for adjustment.

(d) X-ray Apparatus

The X-ray apparatus used in this research work is known commercially as Fedrex and was manufactured by the Carl Drenck X-ray Laboratories in Copenhagen, Denmark. The apparatus consisted of two separate units, namely, the tank unit which contained the high tension filament transformer and X-ray tube, and the control box which contained the switches, controls and measuring devices. The apparatus was operated on 110 volts at 60 cycles with a power consumption

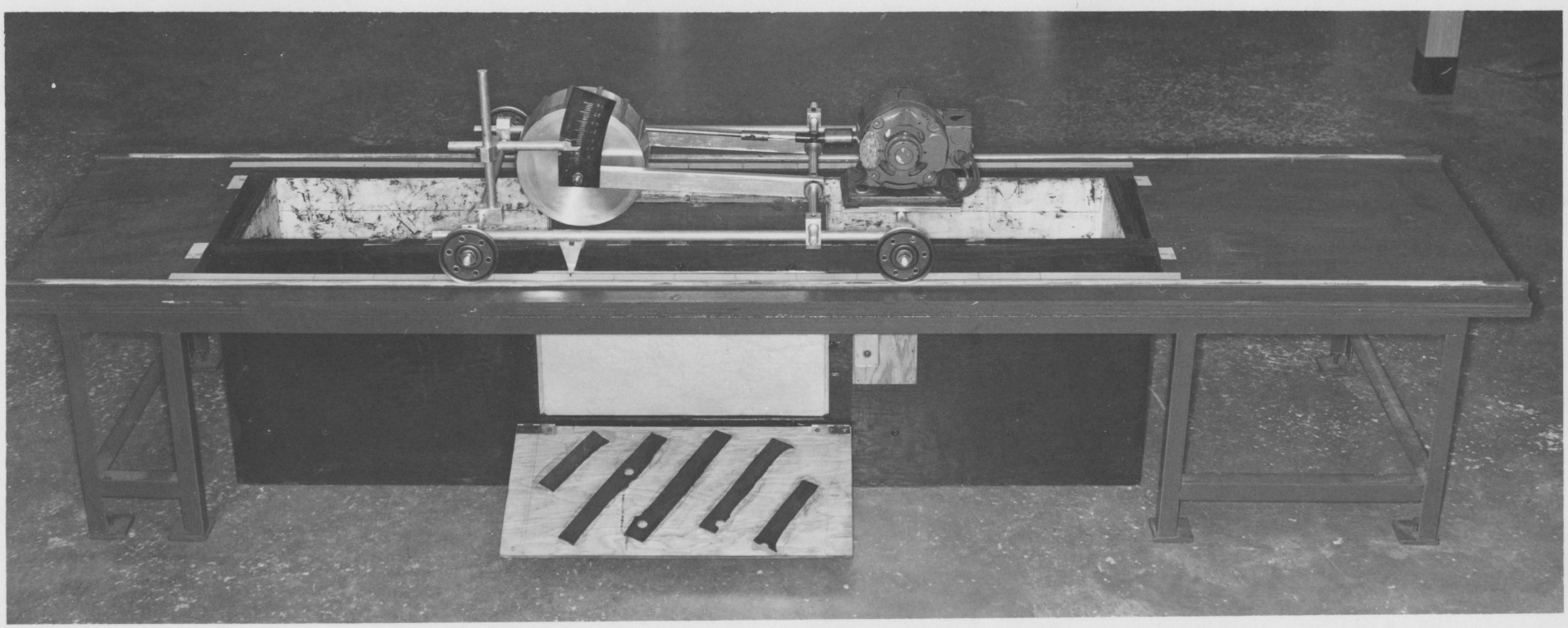

Fig. 7 Test Bin and Track Unit

of 1.5 kilovolt-amps. The voltage supply to the tube was controlled; two ranges permitted the voltage to be regulated steplessly from 30 kilovolts to 100 kilovolts and from 70 K.V. to 130 K.V. It was possible to regulate the tube current without interruption, from 0 to 4 milliamps. A timer, functional for periods of up to 5 minutes, was located on the control unit. At the end of the set time, the unit was automatically switched off. The timer was not used for periods less than 15 seconds as it was very coarse.

The anode angle was approximately 20° and, by using the principle of line focus, an effective focal spot of 1.5 mm. was obtained. An illustration of a line focus tube, showing the relationship between the actual focal spot and the effective focal spot as projected from 20° anode, is shown in Fig. 8 (After Kodak, 1957).

The tank unit emitted considerable stray radiation and, for reasons of safety, was placed in a 1/8 inch thick lead enclosure. Before modifications, the tank unit weighing 50 pounds, was 14 inches long by 9 inches wide by 9 inches high. After modifications, the tank unit weighed 100 pounds and had dimensions of 16 3/8 inches long by 13 inches wide by $10\frac{1}{4}$ inches high.

The exposure time for X-ray film was critical and could not be controlled by the timer on the control unit;

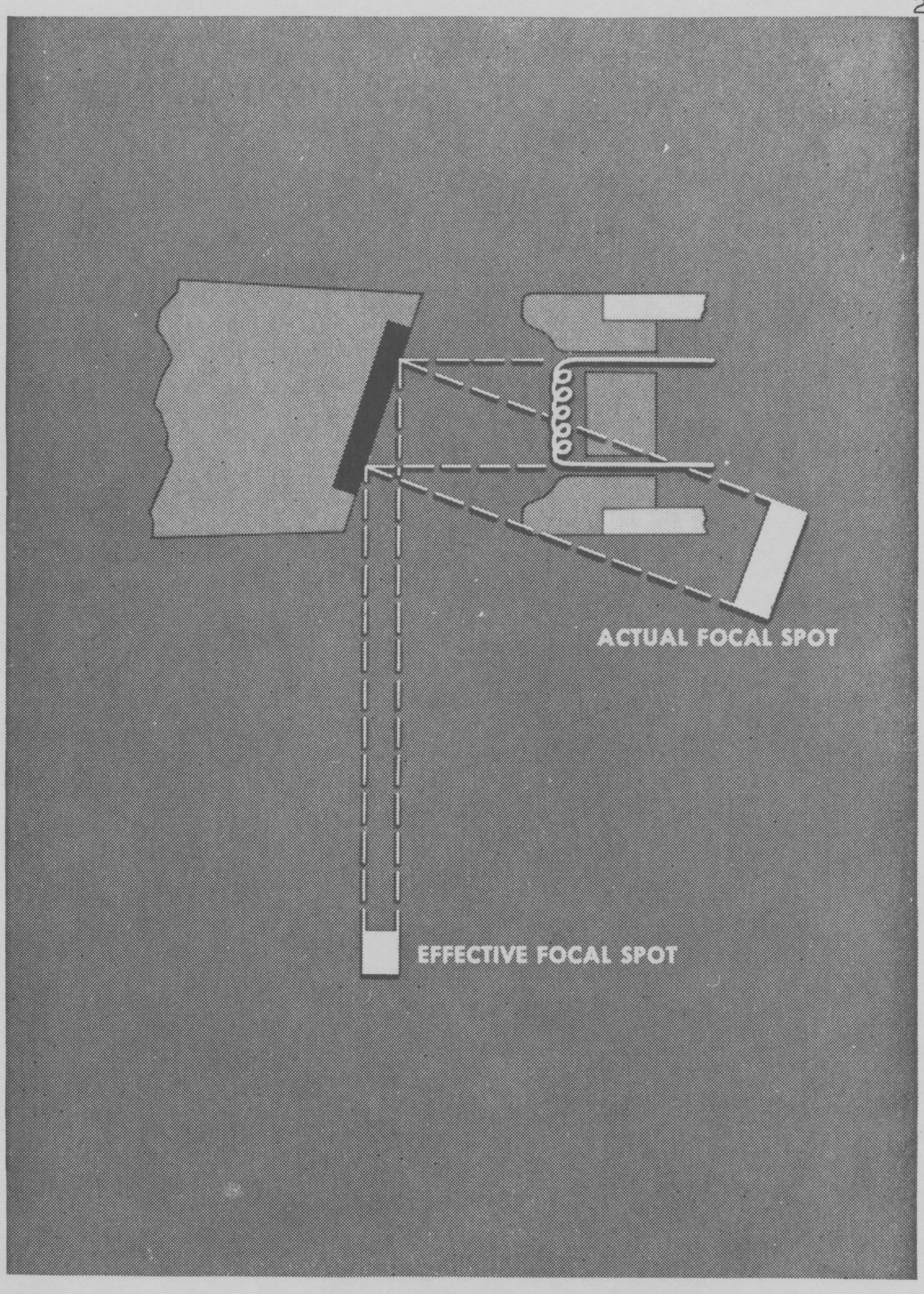

-Diagram of a line-focus tube depicting relation between actual focal spot (area of bombardment) and effective focal spot, as projected from a 20° anode.

FIG. 8 AFTER KODAK (1957)

for this reason, a 6 inch by 6 inch by $\frac{1}{2}$ inch thick lead shutter was added to the tank unit. The exposure time on the film could be controlled by raising and lowering the shutter when the timer was by-passed. This unit can be compared to a camera, and is referred to as an X-ray camera.

(d) X-ray Film, Exposure Holders and Developing Solutions

The choice of X-ray film was made after a series of tests were conducted by North American Inspection Services of Oakville, Ontario. The examination of radiographs, taken under varying conditions of exposure time and power, led to the selection of an industrial X-ray film known commercially as "Gavert-D10". A shortage of supply, during the course of testing, initiated the use of "Kodak KK" industrial X-ray film. It was found that "Kodak KK" film produced a superior radiograph under similar conditions of testing. Initially, the film was used in exposure holders similar to that shown in Fig. 9 (After Kodak, 1957). A suitable reporduction was not possible at the permissible exposure time (5 seconds) when the film was placed in the exposure holder alone. Although the use of lead foil intensifying screens in exposure holders was not recommended by the manufacturers, their use in this application proved to be satisfactory. The lead foil screens (0.005" thick) were placed on each side of the film before the film was inserted into the exposure holder.

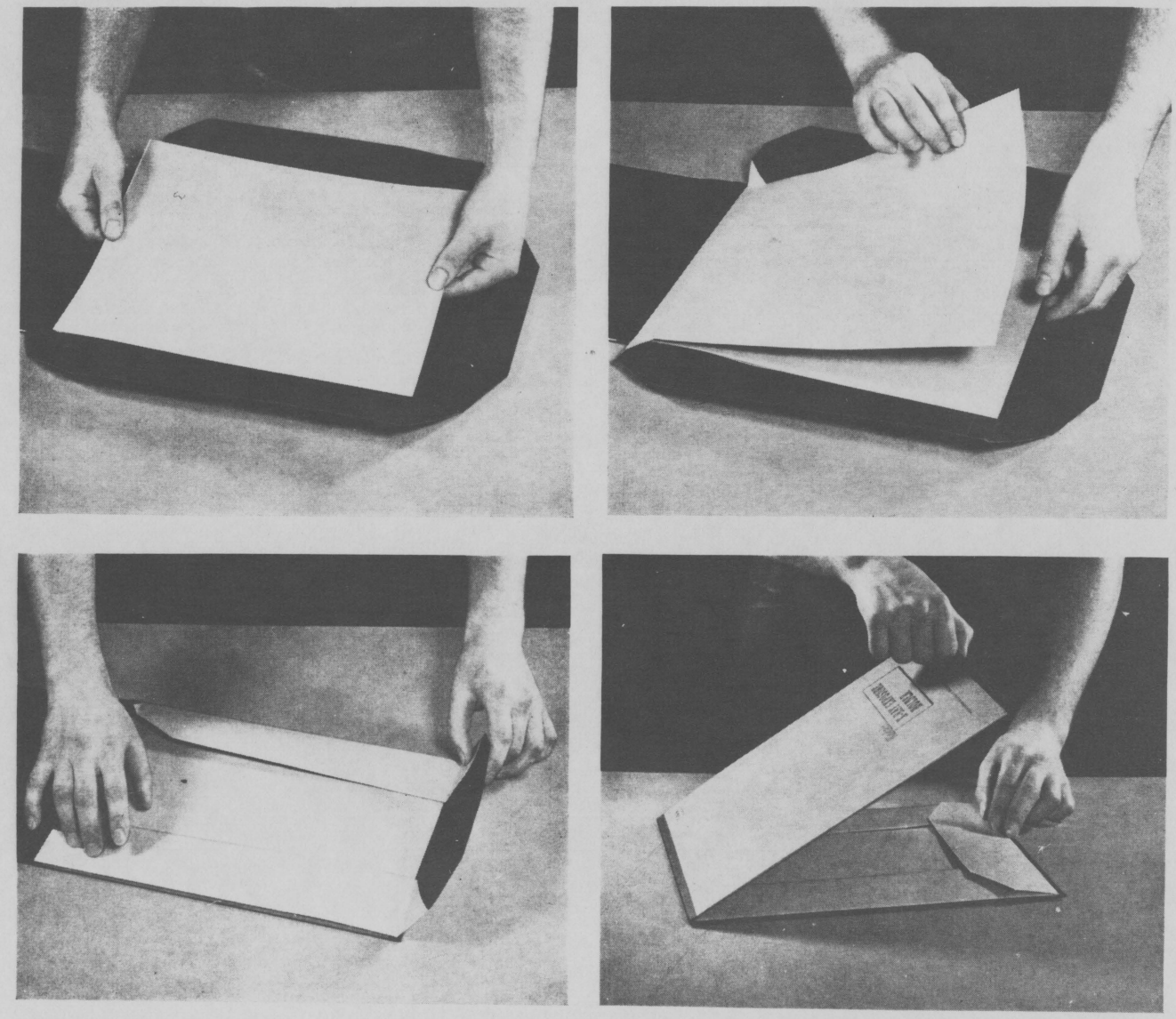

—Method of loading a Kodak X-ray Exposure Holder.

FIG. 9 AFTER KODAK (1957)

The lead foil intensifying screens, in direct contact with the X-ray film, improved the quality of the radiograph by intensifying the primary radiation and absorbing the scattered radiation.

An 8 x 10 inch film size was chosen because it was adequate for recording the movement of the markers. A further advantage in keeping the size of film relatively small was that the quantity of solution required for developing and fixing was not excessive. Four gallons of Gavert liquid developer and the same quantity of fixer were used in order to process six radiographs simultaneously.

(e) Markers

The markers which were used to determine the deformations were constructed from a length of brass rod having a square cross-section with dimensions of one cm. to a side. The rod was machined so that the cross-section had the shape of a cross with four legs of equal length; the legs of each cross were machined to a width of 1/16 of an inch. A cut-off operation produced markers which were 1/16 of an inch thick. Brass was selected rather than lead because of the ease in machining brass.

A locating grid was pasted on one lucite window of the bin; this grid was constructed in the form of one inch squares with 0.015 inch diameter solder. Using this

grid, it was possible to locate the brass markers on the X-ray film. A door, constructed from $\frac{1}{4}$ inch plywood, closed over the window which contained the solder grid. Rubber pads on the door ensured that the X-ray film holder was properly located each time a radiograph was taken. A photograph showing a view of the test bin with the door open is shown in Fig. 7. A radiograph showing the markers in the peat sample is shown in Fig. 10. The markers with three legs (Fig. 10) were off-set from the centre-line of the wheel to record movements on another plane. The data was not used in this thesis.

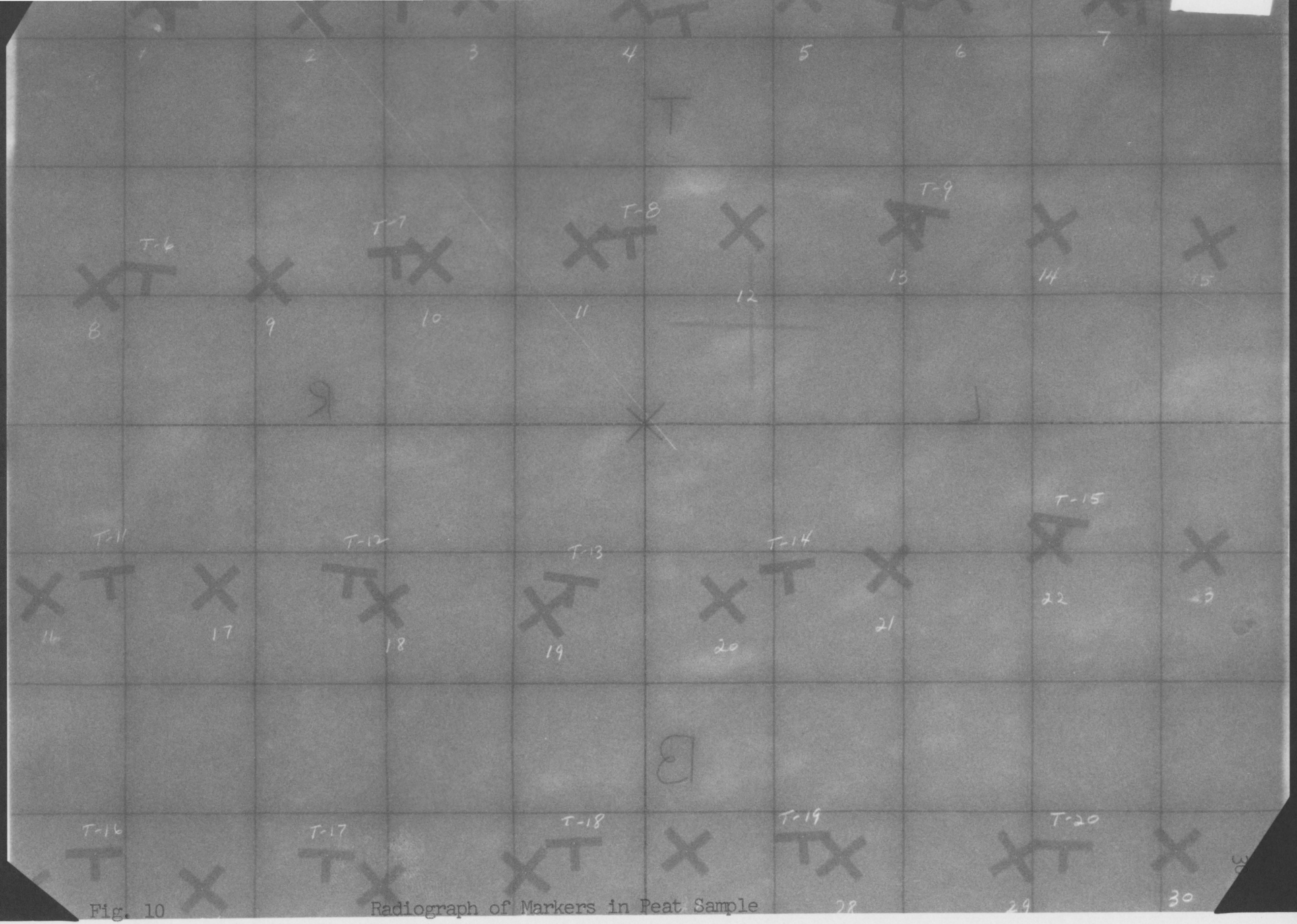

Fig. 10 Radiograph of Markers in Peat Sample

CHAPTER V

TESTING PROCEDURE

(a) Sample Preparation

The sample of peat which was obtained from the field, was passed through a #4 sieve (U.S. Standard), air dried to a moisture content of approximately 660% of the dry weight and stored in a humid room in closed plastic containers. Before each test, the peat in each container was thoroughly mixed to ensure that the sample was homogeneous.

The markers were placed in the proximity of the plexiglass window where they would appear on the radiograph. The brass markers were placed with the cross in a vertical plane along the centre-line of the test bin. A template was used to place the brass markers in the peat. This template consisted of two pieces of 1/8 inch plexiglass, $\frac{1}{2}$ inch wide and 12 inches long, with spaces at the ends. The markers were held between the two pieces of plexiglass. To ensure that the markers maintained their positions while in the template, a film of silicone stopcock grease was applied to the markers to make them adhere to the template. The horizontal spacing of the markers was not critical but an attempt was made to use a regular spacing of one inch.

The markers were imbedded in the peat by placing the template along a guide line and pushing the markers into the peat with a plate which was made to fit between the sides of the template. Four levels of markers were placed in the peat at approximately 1½ inch intervals. After positioning the final series of markers, the test bin was over-filled and the excess peat was removed with a straight edge. Upon completion of the test, the markers were removed from the peat by passing that portion of the sample which contained the markers through the sieve.

(b) Positioning of Track and X-ray Unit

The track unit which carried the wheel was completely independent of the test bin and was positioned and levelled after the test bin was filled. Guide marks on the track unit allowed the test bin to be positioned in the same manner for duplicate tests.

The X-ray apparatus was located 30 inches from the film and the centre-line of the X-ray beam coincided with the centre-line on the film. This positioning procedure was used for radiographs on the horizontal or vertical planes.

(c) Basic Test Procedure

Before each pass of the wheel, an initial radiograph was taken to determine the position of the brass markers before deformation. Radiographs were taken to record the movement

of the markers as the wheel travelled along the test bin. Recordings of time, wheel location and sinkage were taken by photographing the apparatus as the radiograph was being taken. A typical data photograph is shown in Fig. 5.

(d) Detailed Test Procedure for Radiograph on Vertical and Horizontal Planes.

The X-ray film was loaded in a dark room equipped with Kodak "Safelight Filters" (Wratten Series 6B). Although $7\frac{1}{2}$ Watt bulbs were recommended for use with these filters, 15 Watt bulbs were used with no occurance of film fogging.

A lead shield (70 x 34 inches) manufactured for medical X-ray use by Wolf X-ray Products (New York), was used to protect the X-ray camera operator and the X-ray film from direct exposure to radiation during the test. While standing behind the lead shield, the operator of the X-ray camera was able to work in front of the X-ray source and operate the shutter by means of a pully system; in this manner direct exposure to radiation was avoided. This procedure was approved by the Health Physicist at McMaster University. Regular checks, of the radiation dosage accumulated, were made by means of film badges; these checks showed satisfactory working conditions.

When the lead shutter on the X-ray camera was closed, there was some scatter radiation detectable, but not enough

to fog the film. It was during this period that the film holders were positioned in the test bin.

The X-ray apparatus was set at 130 KV and 4 mA. A five-second exposure time was used for radiographs in the vertical plane. At the beginning of the test, a film holder was placed in position and a radiograph was taken by opening the shutter. The wheel was placed in the test bin and the motor started. After a radiograph had been taken, the lead shutter on the camera was closed. The exposed film holder on the test bin was replaced by an unexposed film holder while the exposed film was kept behind the lead shield.

For radiographs taken in the horizontal plane, the X-ray camera was lifted by means of a chain hoist to a stand above the test bin. A film holder was inserted into a slot located below the peat sample. The same procedure of taking photographs of the apparatus to coincide with the radiographs was used. The only difference in technique was that the shutter was opened and closed by means of an extension bar rather than by a pully system. In addition, an exposure time of 8 seconds was used because of the increase in sample thickness from 8 inches to 10½ inches.

Radiographs, for both the vertical and horizontal planes, were taken at six, approximately equal, intervals.

A typical radiograph for an exposure on the vertical plane is shown in Fig. 10.

(e) Developing Radiographs

The film was removed from the holders in the dark room and placed in hangers similar to that shown in Fig. 11 (After Kodak, 1957). The developing and fixing time was obtained by a trial and error process. Gavert Liquid Developer and Fixer were used the the processing time was 6 minutes for developing and 3 minutes for fixing. After fixing, the radiographs were washed for at least 30 minutes, then dried for several hours.

Identification was made by using a key numbering system. A cellulose tape, which could be marked with a ball pen, was used. It was possible to number and cut the tape into sections under normal light. The exposure holders were arranged in the same sequence as the numbers on tape. The numbers were applied to the film under a "Safelight" and the film was inserted into the numbered exposure holder. The cellulose tape remained in position throughout the developing processes.

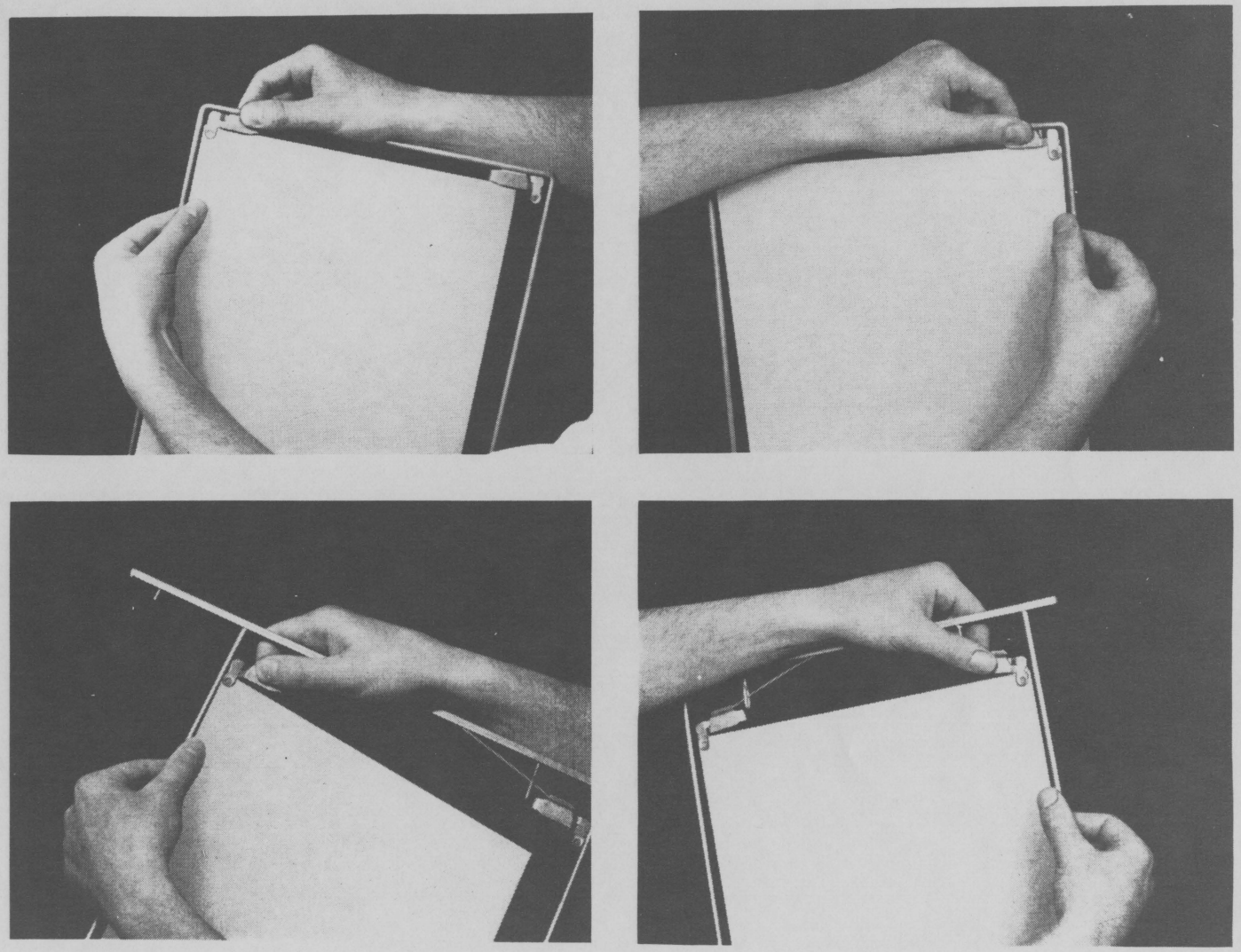

—Method of fastening film on a developing hanger. Bottom clips are fastened first, followed by top clips.

FIG. 11 AFTER KODAK (1957)

CHAPTER VI

THE DETERMINATION OF DEFORMATIONS

The test procedure previously described was used on a total of nine tests. An attempt was made to keep the same moisture content of the sample for each test. It was found that small changes in moisture content influenced the slip and sinkage of the wheel.

For small changes in moisture content, similar movements of the markers were observed. This observation, coupled with the difficulty in controlling slip and sinkage, indicated that the best approach to the problem would be the thorough analysis of one typical test.

The test which was analysed was the eighth performed. This test, at a moisture content of 660% gave a sinkage of 2.35 inches and a slip of 70%. Radiographs for other tests taken on the horizontal plane indicated that the markers which were positioned along the longitudinal centre-line of the wheel remained on this centre-line. To substantiate this radiographs were taken on the horizontal plane for a second pass of the wheel in the eighth test and the markers remained in the centre-line. It was concluded that all the deformations along the centre-line of the wheel were co-planar.

(a) Parallex Corrections

As a radiograph is a shadow picture of an object which has been placed in the path of an X-ray beam, the appearance of the image recorded is influenced by the relative positions of the object, the film, the X-ray apparatus and by the direction of the beam. Corrections for parallex are necessary to compensate for these effects as there is one position at which the true co-ordinates of a marker correspond to the co-ordinates on the X-ray film; this position is the centre of the grid which corresponds to the centre-line of the X-ray beam. A marker which is not in this unique position requires corrections for parallex.

A correction factor was developed by using a method of similar triangles. The X-ray apparatus was located 30 inches from the film during the tests. An image was produced to the same size when the grid of solder, consisting of one inch squares, was placed next to the film. An image with squares of 1.4 inches to a side, was produced when the grid of solder was located $8\frac{1}{2}$ inches from the film. A correction factor (0.857) was calculated for the markers located on the longitudinal centre-line of the wheel (4.3 inches from the film). The same factor was used for both the horizontal and vertical directions on the vertical plane.

Seven radiographs were made while the wheel travelled

the length of the test bin. Thirty markers were observed on each radiograph. The X and Y co-ordinates of the markers were measured from the radiographs. The measured co-ordinates were multiplied by the correction factor (0.857) to obtain the corrected co-ordinates. The depth of the markers below the peat surface was obtained from the corrected co-ordinates by moving the horizontal datum of the grid (centre of the grid) to the top of the peat; the horizontal datum was located at a depth of 5.88 inches below the undisturbed surface of the peat. The true co-ordinates are referenced to the horizontal datum and the vertical centre-line of the radiograph. Table I shows the measured and corrected co-ordinates for seven markers for the test analysed. By moving the horizontal datum to the undisturbed surface of the peat, original positions of the markers were found. The depths to the original positions of the seven markers are given by the last column in Table I.

CHAPTER VII

CORRELATION OF MARKER MOVEMENTS

(a) Relationship between Depth and Size of Cardioid

It was found that the markers moved along a cardioid path and that the size of the cardioid decreased with depth. To determine the relationship between depth and cardioid size, a plot of the marker position with respect to the original position of the marker was made. Each plot consisted of seven points, which were the corrected positions of the marker, corresponding to the various positions of the wheel when the radiographs were taken. Markers, with original positions within 0.10 inches of a horizontal line, were selected and a composite plot of these markers was made. At the lowest level (9 inches below the surface), markers within 0.15 inches were used, as the narrower range provided samples which were too few to be analysed. The increased range had no apparent effect on the composite plot as the movements at this depth were small. A typical composite cardioid is shown in Fig. 12. Four composite cardioids were constructed for depths ranging from 3 to 9 inches; the scale was exaggerated ten times to facilitate plotting and to preserve the accuracy of further measurements.

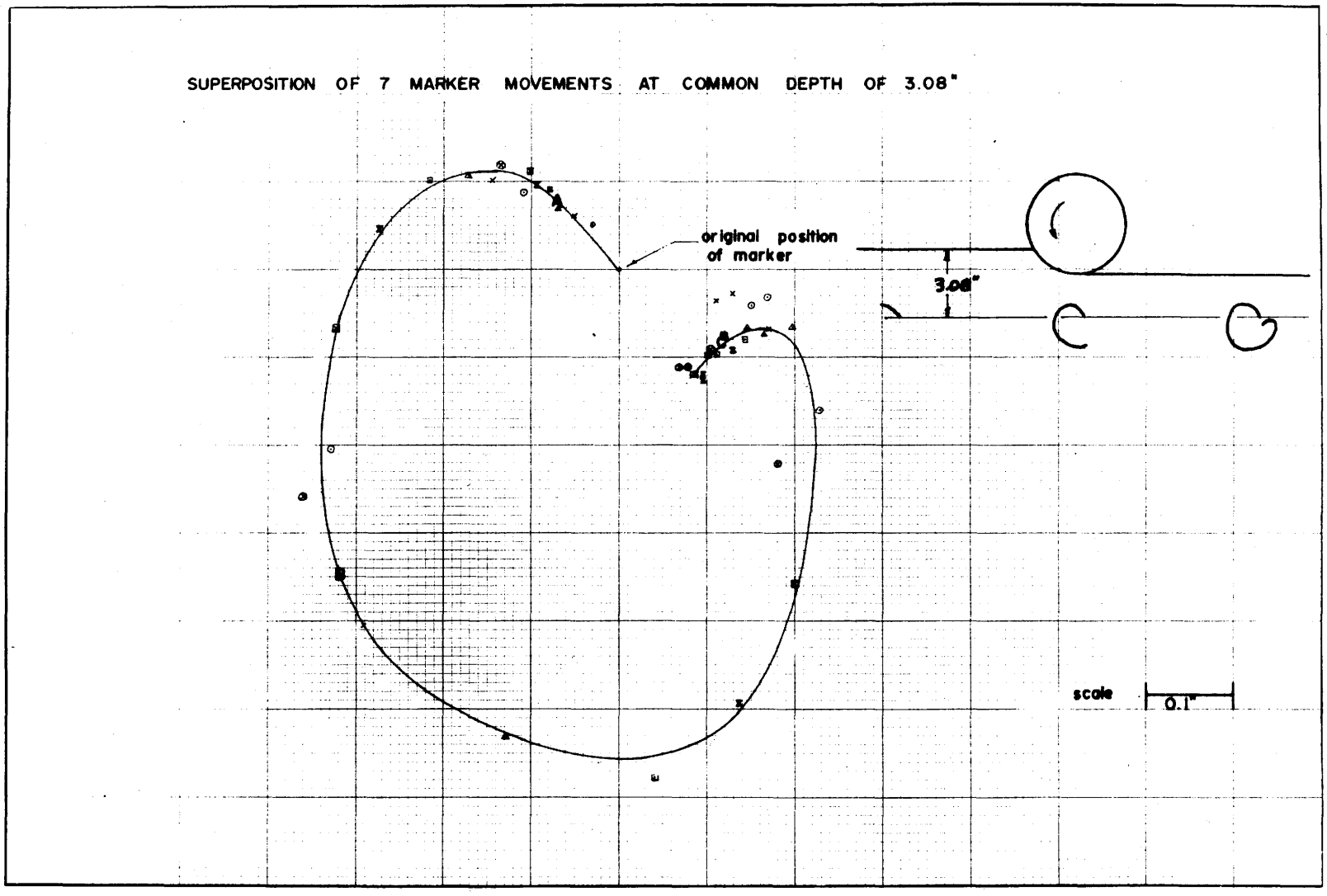

FIG. 12 TYPICAL COMPOSITE CARDIOID

By superimposing the four composite cardioids so that the origins were common, the sizes and shapes of the paths, for chosen depths below the surface of the peat, were obtained by interpolation (Fig. 13).

(b) Relationship Between Position of Wheel and Movement of Marker

A relationship between the wheel position and the movements of the markers was established by measuring the distance travelled by the marker along the cardioid path. The study of the four composite cardioids revealed that the horizontal distances from the centre of the wheel to the original marker positions influenced the magnitudes of movements of the markers. As the wheel approached, the markers which were closest to the wheel moved the most. The markers travelled along cardioid paths as the wheel moved. The influence of the wheel on the markers was felt as the wheel passed over the markers and as the wheel continued to move. At some distance from the marker, this influence diminished to zero. When the total movement around the cardioid path was measured and the movements of the markers were computed as percentages of these total movements, a unique relationship existed between the percentages of total movements and the distance of the wheel from the original marker position. The relationship was independent of depth.

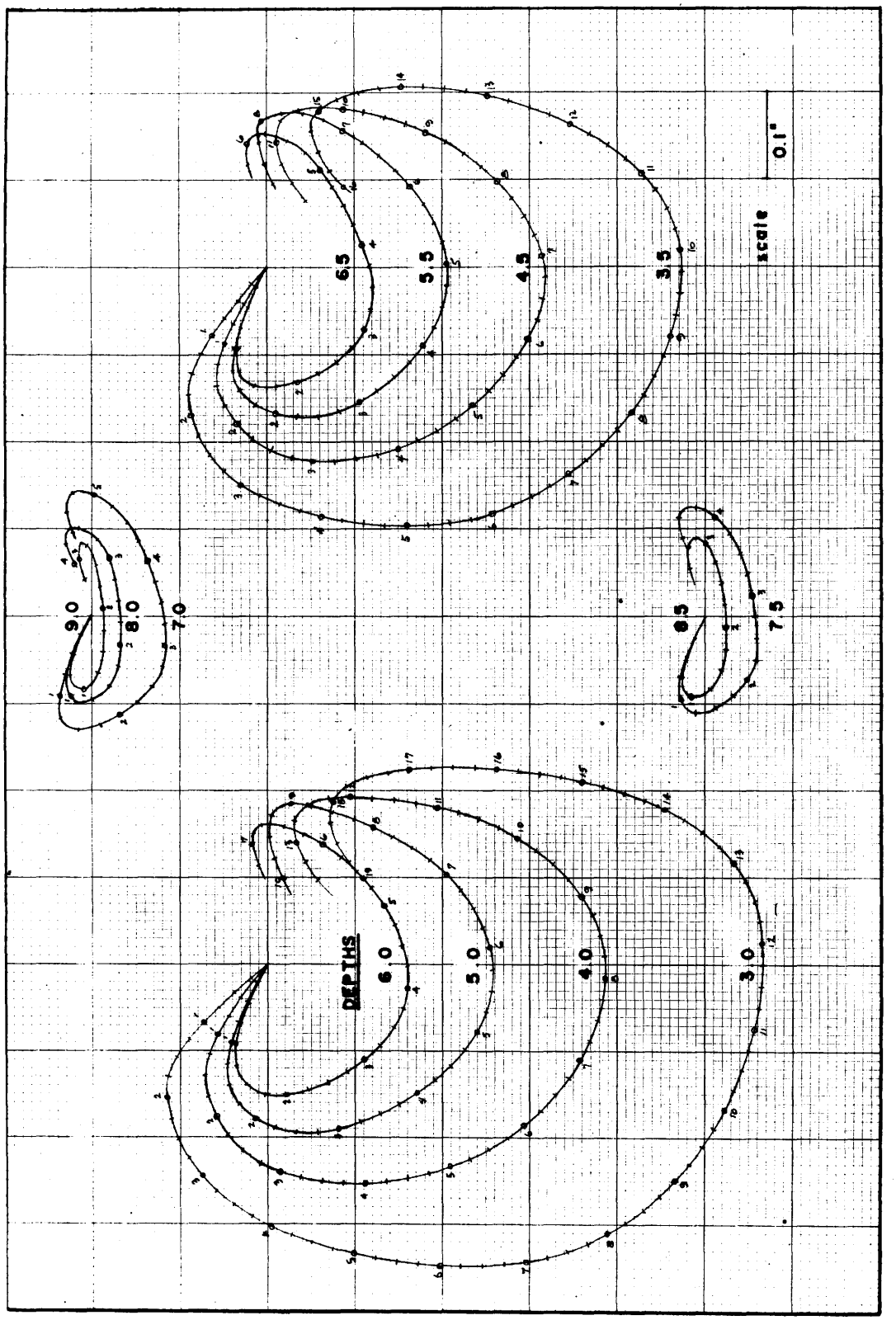

FIG. 13 SHAPES OF CARDIOIDS AT VARIOUS DEPTHS

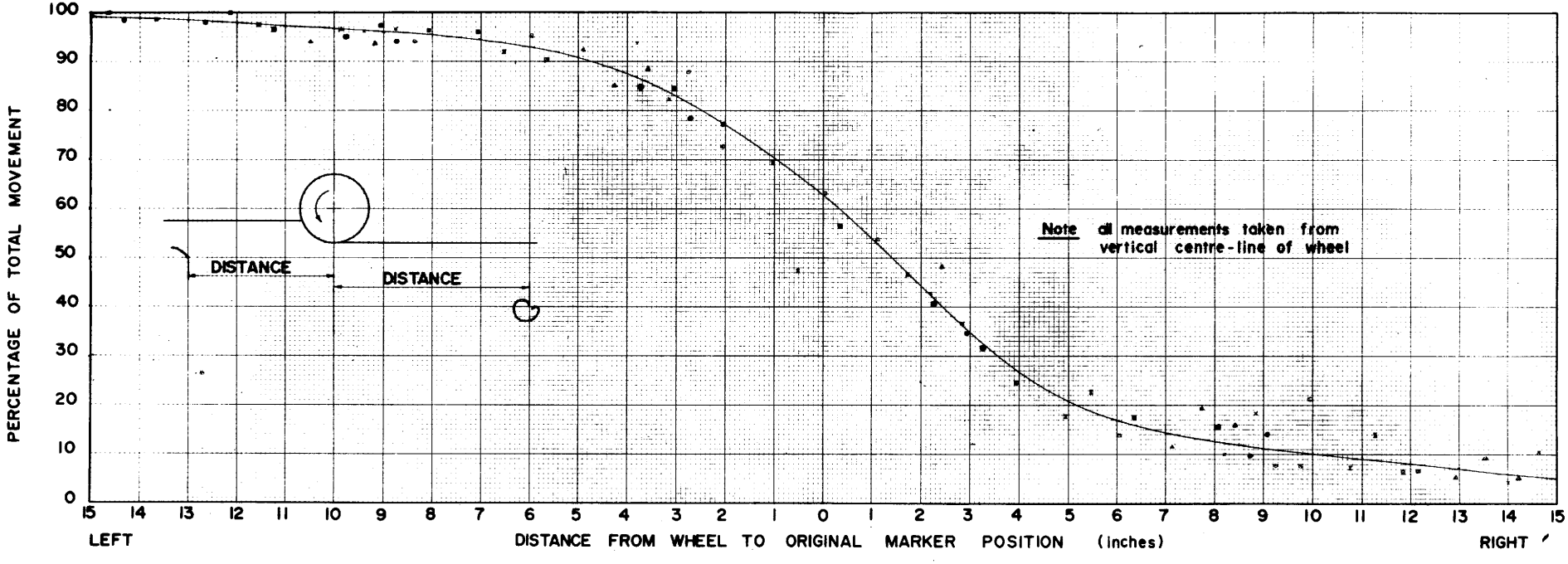

FIG. 14 MOVEMENTS OF MARKERS

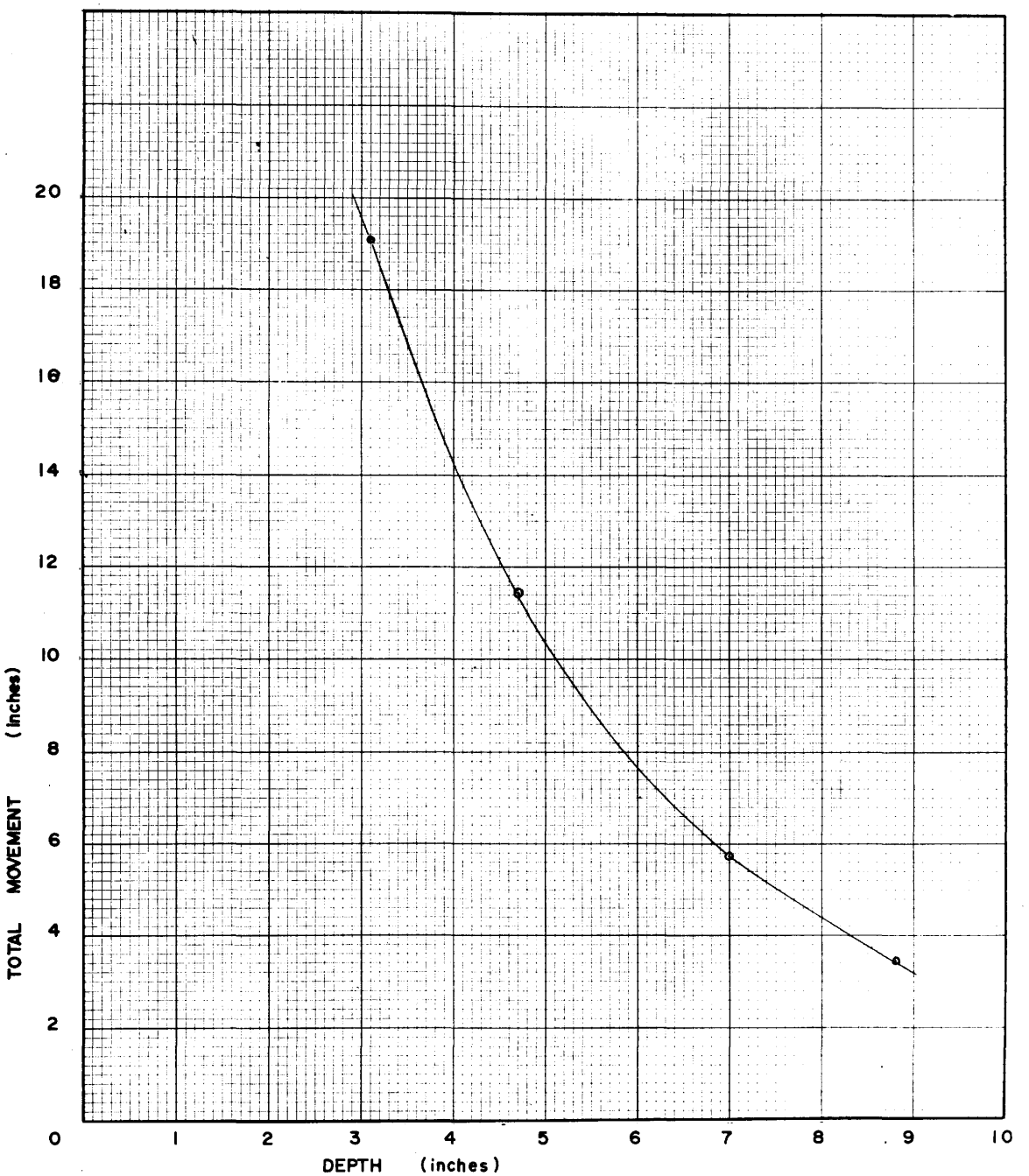

FIG. 15 INFLUENCE OF DEPTH ON TOTAL MOVEMENT

The motion of the wheel was from right to left. Fig. 14 was obtained by plotting the percentages of total movements against the distances from the wheel to the original marker positions for various positions of the wheel.

The data, used to obtain the graph shown in Fig. 14 were based on the four composite plots. As these plots occurred at irregular intervals between 3 inches and 9 inches, an interpolation was required to determine the total movements of markers for any required depth. A graph showing the relationship between the depth and the total distance travelled is shown in Fig. 15.

As the size of the cardioid and the total movement can be determined by interpolation for any depth, the marker position for any location of the wheel can be determined. With this information, it is possible to plot the deformations of a plane on the centre-line of the wheel.

CHAPTER VIII

GRAPHICAL METHOD FOR ANALYSIS OF DEFORMATIONS

The correlation of marker movements showed that the markers behaved in a unique manner. Accordingly, the movements were analysed to determine the relationships of the movements to the stress configurations. The graphical method used to determine, from deformations, the trajectories of the principal stresses was proposed originally by Haefeli (Haefeli, 1944). A translation, in part, of Haefeli's work, including the derivation of the graphical solution used in this thesis is included as Appendix A.

The mechanics of the method, proposed by Haefeli, are described in the following text. Assuming that the soil mass is marked with a regular line network, part of which is shown in Fig. 16 (Appendix A, Fig. 5), the intersection of two lines (AB and CD) is denoted by the point P.

The external forces cause a deformation to take place and the network becomes deformed and moves to a new position which is denoted by the points A', P', B', and C', P', D'. To determine the principal stress directions at the point P, a tangent is drawn to the line A'B' at the point P'. The tangent intersects the line AB at the point T_2. In a similar manner, the tangent drawn to the line C'D' at the

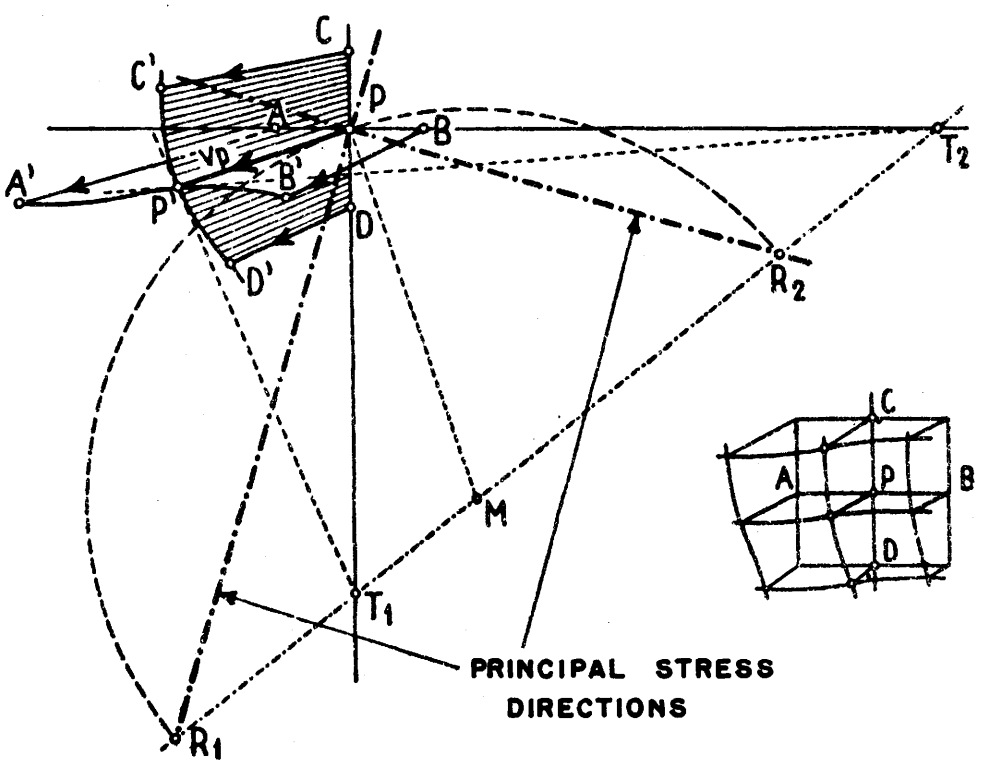

FIG. 16 GENERAL CONSTRUCTION FOR PRINCIPAL STRESS DIRECTIONS

AFTER HAEFELI (1944)

point P' intersects the line CD at the point T_1. A line drawn through the points T_1 and T_2 represents the locus of momentary centres of circles which determine the directions of the principal stresses.

To find the directions of the principal stresses at point P, a line, perpendicular to the flow Vp, is dropped from P to intersect the line T_1T_2 at point M. A circle with centre M and radius MP cuts the line T_1T_2 at R_1 and R_2. The straight lines R_1P and R_2P represent the directions of the principal stresses.

Haefeli stated that the method described is valid only for very small planar deformations of the network. In addition, it is necessary for the network to move in its own plane in such a manner that all points travel in straight lines and at regular spatially distributed distances.

This research work on peat has shown that the marker position can be determined for any depth and for any location of the wheel. An imaginary line network with markers at the nodal points was formed and, therefore, the condition of a regular line network was satisfied. As the wheel approached the network, the deformations were determined by the relative marker movements. The deformed network was established by joining the displaced markers.

For sharply curved flow lines, which were evident in this research, it was suggested by Haefeli that the procedure for finding principal stress directions be used differentially; the condition that the points travelled in straight lines was satisfied. In addition, the condition for regular spatially distributed distances was satisfied by the construction of a new undeformed network after each differential movement.

The cardioids, at various depths (Fig. 13), were drawn five times normal scale for the determination of principal stress directions. A network was constructed on graph paper and the nodal points were assumed to be the positions of the markers. The marker movements were plotted for a chosen wheel interval. Wheel intervals were chosen where the differential movement of the markers could be approximated by straight lines. Haefeli's method was used to determine the principal stress directions for the point under consideration.

For the next position of the markers, a new undeformed network was constructed and the graphical method was repeated. The principal stress trajectories were obtained by drawing curves at the directions of the principal stresses for the points under consideration (Fig. 17).

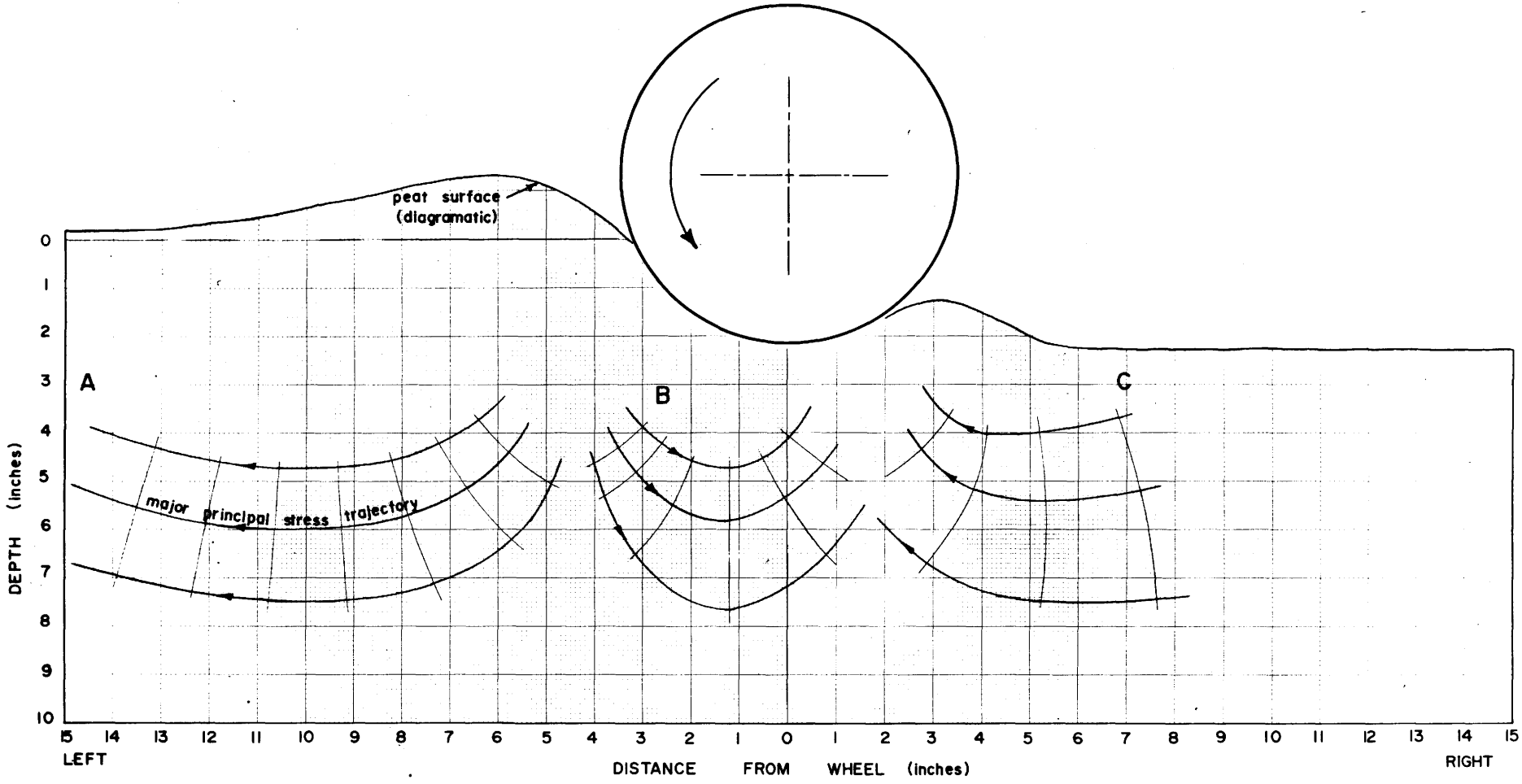

FIG. 17 TRAJECTORIES OF PRINCIPAL STRESSES

The small relative movements of markers presented a problem in determining the location of the points T_1 and T_2 as convergence of the tangents (drawn through P') with their respective axis usually occurred at great distances (up to 4 feet) from the nodal point P (Fig. 16). For this reason, the accuracy of the method was questioned and the resulting principal stress trajectories (Fig. 17) present an approximation to the true stress trajectories.

CHAPTER IX

ANALYSIS OF DEFORMATIONS

It was established that markers in peat follow cardioid paths. An inspection of the cardioids (Fig. 13) revealed that the influence of the bottom of the test bin was significant at the lower depths. The cardioids which were formed near the surface of the peat had rounded shapes, while those near the bottom were flattened. Substantial variations in percentages of total movements were not apparent from the plot of marker movements (Fig. 14). The movements of the markers were related to the positions of the wheel; an account of these movements was made.

As the wheel approached a marker, movements of the marker upward and away from the wheel were observed (e.g. marker at A, Fig. 12 and Fig. 17). This movement was attributed to a wave which preceeded the wheel. An examination of the principal stress trajectories (Fig. 17) revealed that the wave was initiated at the leading edge of the wheel. Further examination of the stress trajectories showed that the wave action was followed by a displacement due to the load and rotation of the wheel (e.g. marker at B, Fig. 17). This is substantiated by observing the position of the marker on the composite cardioid (e.g. marker at B, Fig. 12).

A study of the plots (Fig. 12 and Fig. 17) indicated that the final movement was due to the generation and dissipation of a wave behind the wheel (e.g. marker at C, Fig. 12 and Fig. 17). The principal stress trajectories (Fig. 17) were considered to be an approximattion to the true trajectories, but they provided an aid in describing the movements of the markers.

The angle of internal friction for amorphous granular peat was assumed to be zero ($\phi = o$). This assumption permitted the surfaces of maximum shear to be determined approximately. In soil mechanics, the angle between the plane of major principal stress and the direction of maximum shear is given as $\alpha = 45° + \frac{\phi}{2}$. The angle α is 45° for $\phi = o$.

The angles between the directions of principal stresses (Fig. 17) were bisected to determine the surfaces of maximum shear (Fig. 18). With the determination of the surfaces of maximum shear, an analysis may be approached with the theories presently available in soil mechanics. The analysis can be compared to slope stability where the internal forces of shear on the surfaces of maximum shear can be equated to the external forces acting on the soil mass.

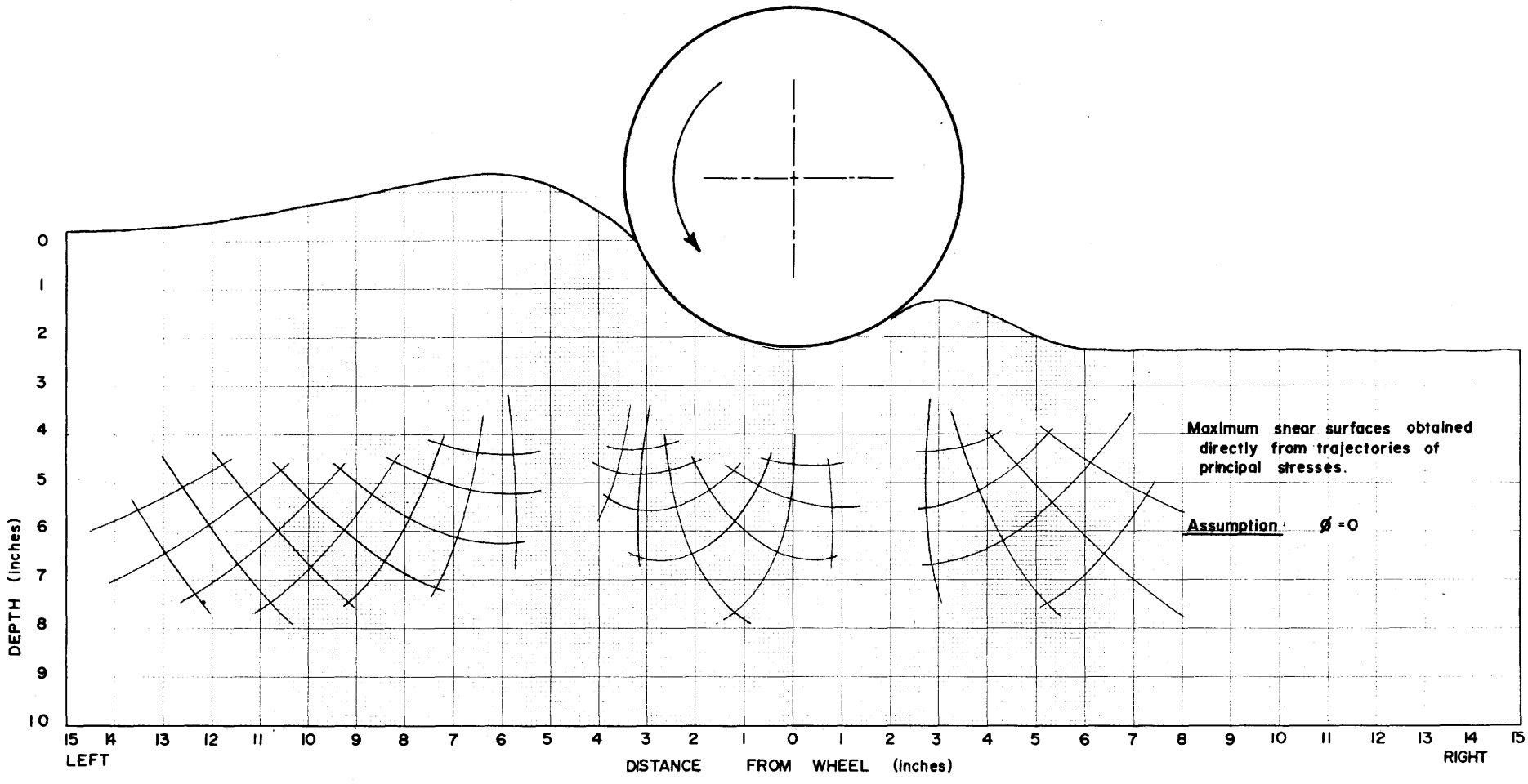

FIG. 18 SURFACES OF MAXIMUM SHEAR

CHAPTER X

CONCLUSIONS

A fundamental approach to the problem of vehicle mobility, by the study of deformations and stress trajectories of the soil as a wheel moved, has been described.

A driven rigid wheel was constructed to run over a sample of amorphous granular peat. Metal markers were placed throughout the peat and a record of their movements was obtained as the wheel travelled over the peat. The movements of the markers were recorded on films by using an X-ray technique.

The markers were observed to move in cardioid paths as the wheel travelled over the peat. A unique relationship existed between the positions of the wheel and the movements of the markers; this relationship established the movements of markers at any position within the peat.

The trajectories of the principal stresses were determined by a graphical method. The stress trajectories, although considered to be approximate, aided the analysis of marker movements. The surfaces of maximum shear were obtained directly from the stress trajectories by assuming an angle of internal friction for amorphous granular peat to be zero. The shear surfaces obtained directly from the

stress trajectories are shown in Fig. 18. A knowledge of the surfaces of maximum shear may permit an analysis of vehicle mobility problems to be approached with the theories presently available in soil mechanics.

The surface of maximum shear were reconstructed (Fig. 19) by observing the trends established in the original determination (Fig. 18). The resulting surfaces of maximum shear resemble those associated with slope stability problems in soil mechanics. The problems of vehicle mobility and slope stability become analogous as the surfaces of maximum shear and the shear stresses are related to the forces acting on the soil mass.

The determination of deformations in soil is a fundamental approach to the vehicle mobility problem. It was shown that deformations within this soil can be determined. The task which awaits future researchers is to verify and improve on the methods used to evaluate deformations.

Initially, an improvement in equipment is necessary. Soil containers which are much larger should be used to minimize the effects of the walls and bottom. A large number of tests, performed with a variety of soil conditions and wheel configurations, are necessary to establish the existence of a relationship between wheel positions and marker movements.

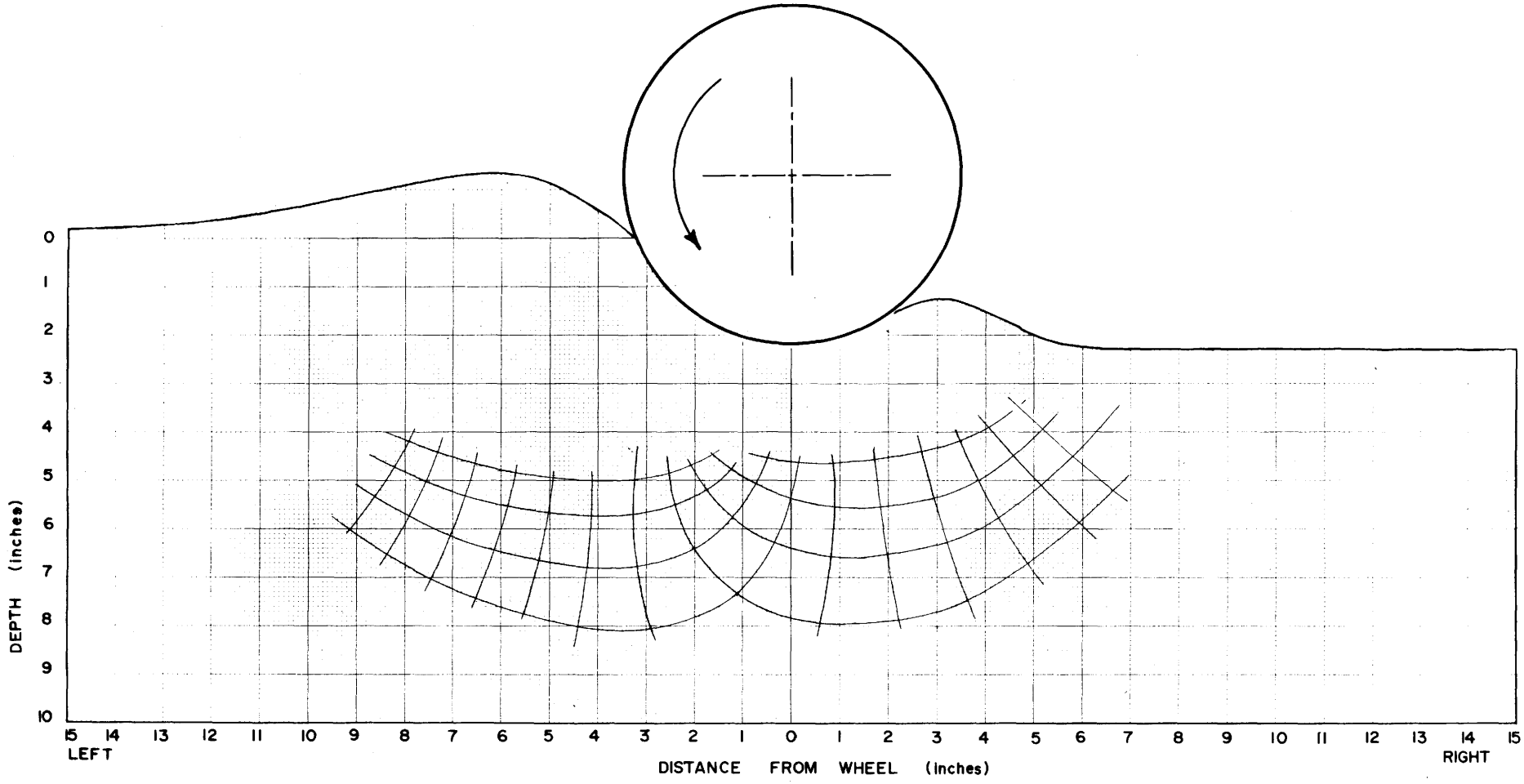

FIG. 19 RECONSTRUCTED SURFACES OF MAXIMUM SHEAR

A study of the methods for determining principal stress and strain directions, is needed to determine which methods are acceptable.

The mutual examination of pressure cell and deformation data is necessary to establish the magnitudes and directions of the principal stresses. This information may be helpful for establishing the relationships between soil and vehicle; the behaviour of the vehicle should be established in terms of the soil-vehicle relationships.

REFERENCES

Adams, J.I. (1961).
Laboratory compression tests on peat. Proc., 7th. Muskeg Research Conference, National Research Council (Canada), Associate Committee on Soil and Snow Mechanics, Technical Memorandum No. 71, pp 36-54.

Anderson, K.O. (1962).
Muskeg studies in Alberta. Soil Foundation and Materials Exploration Methods, Application and Evaluation, National Research Council (Washington, D.C.), Highway Research Board Bulletin No. 316.

Bekker, M.G. (1956).
Theory of Land Locomotion. University of Michigan Press, Ann Arbor.

Bekker, M.G. (1960).
Off-The-Road Locomotion. University of Michigan Press, Ann Arbor.

Bekker, M.G. (1961).
Evaluation and selection of optimum vehicle types under random terrain conditions. Proc., 1st International Conference on the Mechanics of Soil Vehicle Systems, Paper No. 43.

Brawner, C.O. (1958).
The muskeg problem in B.C. highway construction. Proc., 4th Muskeg Research Conference, National Research Council (Canada), Associate Committee on Soil and Snow Mechanics, Technical Memorandum No. 54.

Cooper, A.W. et al. (1957).
Strain gauge cell measures soil pressure. Agricultural Engineering, April.

Dickson, W.J. (1962).
Ground vehicle mobility on soft terrain. Journal of Soil Mechanics and Foundations Division, Proc., American Society of Civil Engineers, August.

Eden, W.J. and Kubota, J.K. (1962).
Some observations on the measurement of sensitivity of clays. National Research Council (Canada), Division of Building Research, Research Paper No. 157.

Freitag, D.R. and Knight, S.J. (1961).
Stresses in yielding soils under moving wheels and tracks. United States Army Engineers, Waterways Experiement Station, Corps of Engineers, Vicksburg, Mississippi.

Freitag, D.R. and Green, A.J. (1961).
Distribution of stresses on an unyielding surface beneath a pneumatic tire. United States Army Engineers, Waterways Experiment Station, Corps of Engineers, Vicksburg, Mississippi.

Goodman, L.J. and Lea, C.N. (1961).
Effects of remoulding on soil values related to vehicle mobility. Proc., 1st International Conference on the Mechanics of Soil-Vehicle System, Paper No. 4.

Green, A.J. (1962).
Some fundamental mobility studies. United States Army Engineers, Waterways Experiment Station, Corps of Engineers, Vicksburg, Mississippi.

Haefeli, R. (1944).
Erdbaumechanische Problem im Lichte der Schneeforschung. Leeman and Company, Zurich.

Hanrahan, E.T. (1954).
An investigation of some properties of peat.
Geotechnique, Vol. IV, p. 108.

Kodak Company (1957).
Radiography in Modern Industry. Eastman Kodak Company, Rochester.

Krzywicki, H.R. and Wilson, N.E. (1964).
Viscosity measurements to determine the shear strength of peat. Proc., 10th Muskeg Research Conference, National Research Council (Canada), Associate Committee on Soil and Snow Mechanics.

MacFarlane, I.C. (1958).
Guide to a Field Description of Muskeg. National Research Council (Canada), Associate Committee on Soil and Snow Mechanics, Technical Memorandum No. 44.

MacFarlane, I.C. and Rutka, A. (1962).
An evaluation of pavement performance over muskeg in Northern Ontario. Soil Foundation and Materials Exploration Methods, Application and Evaluation, National Research Council (Washington, D.C.), Highway Research Board Bulletin No. 316.

Markowsky, M. and Adams, J.I. (1960).
Anchorage of transmission towers in muskeg. Ontario Hydro Research News, Vol. 12, No. 4, pp 24-29.

McKibben, E.G. (1938).
Some kinematic and dynamic studies of rigid transport wheels for agricultural equipment. Iowa State College of Agriculture and Mechanic Arts, Ph.D. Thesis No. 404.

McKibben, E.G. and Davidson, J.B. (1940).
Transport wheels for agricultural machines - Effect of outside and cross-sectional diameters on the rolling resistance of pneumatic implement tires. Agricultural Engineering, Journal of American Society of Agricultural Engineers, Vol. 21.

Meyer, M.L. (1963).
Interpretation of surface-strain measurements in Terms of homogeneous strains. Experimental Mechanics, Vol. 3, No. 12, pp 294-301.

Monaghan, B.M. (1963).
Muskeg and the Quebec North Shore and Laborador Railway. The Engineering Journal, Vol. 46, No. 3, pp 35-40.

Nuttall, C.J. (1949).
Scale model vehicle testing in non-plastic soil. Experimental Towing Tank, Stevens Institute of Technology, Report No. 394.

Radforth, N.W. (1952).
Suggested classification of muskeg for engineering. The Engineering Journal, Vol. 35, No. 11, p. 1194.

Radforth, N.W. (1957).
Correlation of palaeobotanical and engineering studies of muskeg in Canada. Proc., 4th International Conference on Soil Mechanics and Foundation Engineering, Vol. I, p. 93.

Reece, A.R. and Wills, B.M.D. (1961).
Forced-slip wheel and track tester. Proc. 1st International Conference on the Mechanics of Soil-Vehicle Systems, Paper No. 25.

Ripley, C.F. and Leonoff, C.E. (1961).
Embankment settlement behaviour on deep peat. Proc. 7th. Muskeg Research Conference, National Research Council (Canada), Associate Committee on Soil and Snow Mechanics, Technical Memorandum No. 71, pp 185-204.

Roscoe, K.H. et al. (1963).
The determination of strains in soil by using an X-ray method. Civil Engineering and Public Works Review, No. 7, pp 874-876.

Schroeder, J. and Wilson, N.E. (1962).
The analysis of secondary consolidation of peat. Proc., 8th Muskeg Research Conference, National Research Council (Canada), Associate Committee on Soil and Snow Mechanics, Technical Memorandum No. 74.

Thomson, J.G. (1958).
Vehicle mobility performance in muskeg - a preliminary report. Proc., 4th. Muskeg Research Conference, National Research Council (Canada), Associate Committee on Soil and Snow Mechanics, Technical Memorandum No. 54.

Thomson, J.G. (1960).
Vehicles in muskeg. The Engineering Journal, Vol. 43, No. 5, pp 73-78.

Thomson, J.G. (1961).
Vehicle design from field test data. Proc., 1st. International Conference on the Mechanics of Soil-Vehicle Systems.

Trabbic, G.W. et al. (1959).
Measurement of soil-tire interface pressures. Agricultural Engineering, November.

Uffelman, F.L. (1960).
Fighting vehicles research and development establishment. Tripartite Working Group on Ground Mobility. Defence Research Board (Canada), Department of National Defence, Report on 2nd. Conference.

Vanden-Berg, G.E. et al. (1957).
Soil pressure distribution under tractor implement traffic. Agricultural Engineering, December.

Wilson, N.E. (1963).
Laboratory vane shear tests and the influence of pore-water stresses. Presented at Symposium on Laboratory Shear Testing of Soils, Ottawa under direction of American Society of Testing Materials and National Research Council (Canada).

APPENDIX A

"THE GENERAL DETERMINATION OF PLANAR STRESS CONDITIONS IN PLASTIC BODIES"

A translation from

Erdaumechanische Probleme im Lichte der Schneeforschung

(Problems for Soil Mechanics in the light of Snow Research)

Dr. R. Haefeli

Zurich, 1944

GENERAL DETERMINATION OF PLANAR STRESS CONDITIONS IN PLASTIC BODIES

One group of basic methods in soil mechanics for determining the effective forces includes the classic earth pressure theory which deals with the investigation of the so called limiting states of equilibrium. A second group of methods, which are used for example, to calculate the pressure distribution in the soil below foundations was formulated by Boussinesq, and makes use of the mathematical elastic theory to reach, in cases with simple boundary conditions, the solution for the states of stresses. The simple fact that the mechanical properties of a compressible material allow it to compact or compress continuously, shows that the conditions of the mathematical elastic theory are not satisfied.

More and more the need for calculation methods arise, which comply with the actual plastic behaviour of the material. Nature offers us in the form of hard snow and ice a material which allows us to study the plastic processes in an ideal manner. It is, therefore, no accident that the analysis of the equilibrium of snow cover has led to certain solutions which have a general significance. One of those solutions could be given, for example, for the stress condition

of a plastic, plane, parallel layer of snow under its own weight. First of all, however, certain assumptions about the deformation state must be made. Because of this special deformation state, the directions of the principal stress trajectories could be found. Before we try to take the given method for the determination of stress trajectories for snow more general, the above solution which has already been published is repeated as an introduction.

If one cuts out of a flat continuous slope, a prismatic particle element with depth 1, length 1, and height y, the equilibrium of this element demands that an opposite equal component P_X be parallel to the slope area and the resulting stress P_Z be vertical (Fig. 1). The two components of P_Z are calculated as normal stress and shear stress as follows:

$$(1)\quad \sigma_y = y\,\gamma_s \cos\psi = z\,\gamma_s \cos^2\psi$$

$$(2)\quad \tau_x = y\,\gamma_s \sin\psi = z\,\gamma_s \sin\psi\cos\psi$$

For the components of P_X one knows, however, only their direction and not their value. This special case, known as Rankine's stress state in earth pressure theory, was solved by Rankine with the assumption that the particle of earth under consideration is everwhere in the limiting state of equilibrium, i.e. that through each point inside the earth element, there exists a failure plane for which Newton's classic law of friction is valid. With this assumption, Rankine calculated the major principal stresses and their

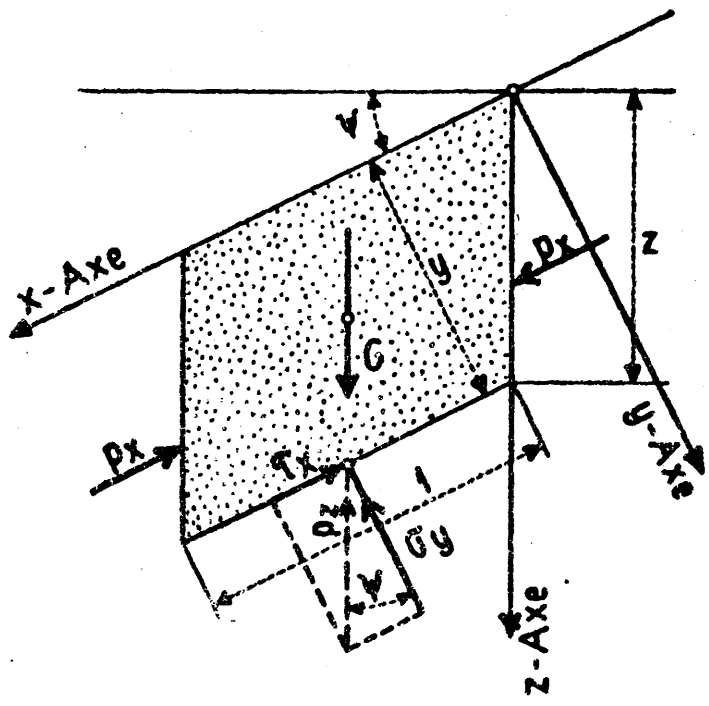

Element of a Body.

Fig. 1

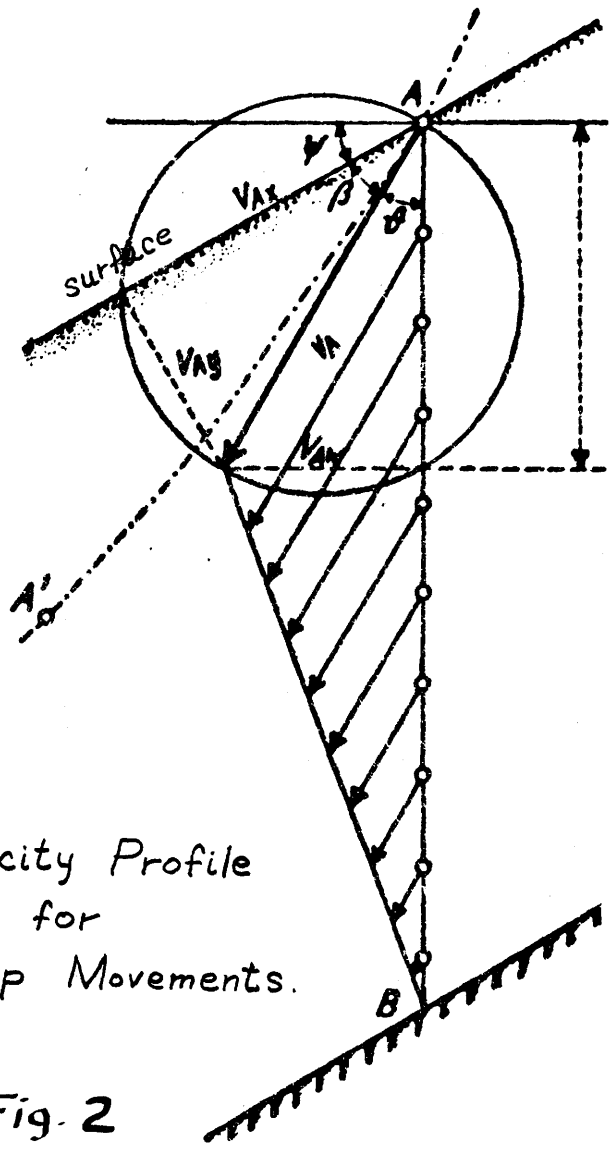

Velocity Profile
for
Creep Movements.

Fig. 2

directions. (Rankine's formulae).

For continuous slopes, which is the normal case for snowfields, which are not in the limiting state of equilibrium and are neither without cohesion nor do they follow Newton's law of friction, a more general solution of Rankine's stress state had to be found. In the work "Snow Mechanics" it has been shown, that a solution for plastic materials such as snow exists and can easily be found when consideration is given to the deformed state of the plane parallel layer underlain by a rigid subsoil, i.e. the creep movement can be characterized by a triangular velocity profile with parallel creep velocities. (Fig. 2).

First of all, a simple observation shows that for the above assumptions about the creep movement, the direction of the principal stresses is also clearly given. (Fig. 3). The considered creep process distinguishes itself by the fact that each straight line, which is thought of as a connecting line of material points (snow crystals) that lie in the plane of the figure, stays a straight line during the plastic deformation, and performs a rotation about its point of intersection with the rigid ground. This is also true for the cords PE and PD of the semi-circle drawn through P. The centre point M lies on the line which is perpendicular to the creep direction and which passes through point P.

The right angle DPE which is enclosed by both cords, undergoes no changes of periphery angle, if point P moves slightly in the direction V. This is only possible if in both perpendicular directions, PE and PD, no shearing stress is effective. From this observation, their identity, with the principal stress directions is evident. By the definition of the ideal plastic body, each, however, small, shear stress creates a steadily progressing angle deformation.

Through the known stresses (σ_y, τ_x) and the direction of the main stresses, the stress state at point P is now completely determined. The Mohr's stress circle can now be constructed according to Fig. 3a. Proceeding from point P one obtains, by plotting the stress values σ_y and τ_x, the first point P' of the required stress cirlce. One draws the line P'F, which is inclined at the known angle α about the horizontal axis and is, at the same time, the cord of the stress circle. The centre C of the stress circle can easily be found. According to Fig. 3, one obtains from the sum of angles in AMPD the following value for $\measuredangle\alpha$: $\measuredangle MDP = \measuredangle MPD = \alpha$

$(90° - \beta) + 2\alpha = 180°$ $\quad\therefore\quad \alpha = 45° + \beta/2$

From this it follows for the $\measuredangle CP'G$ in Fig. 3.

$\measuredangle CP'G = 2\alpha - 90° = \beta$.

One can, therefore, obtain the centre C of the Mohr's circle directly by plotting the creep angle β starting from the vertical at point P' and bringing it to cut the horizontal axis through P. The two main stresses, which characterize

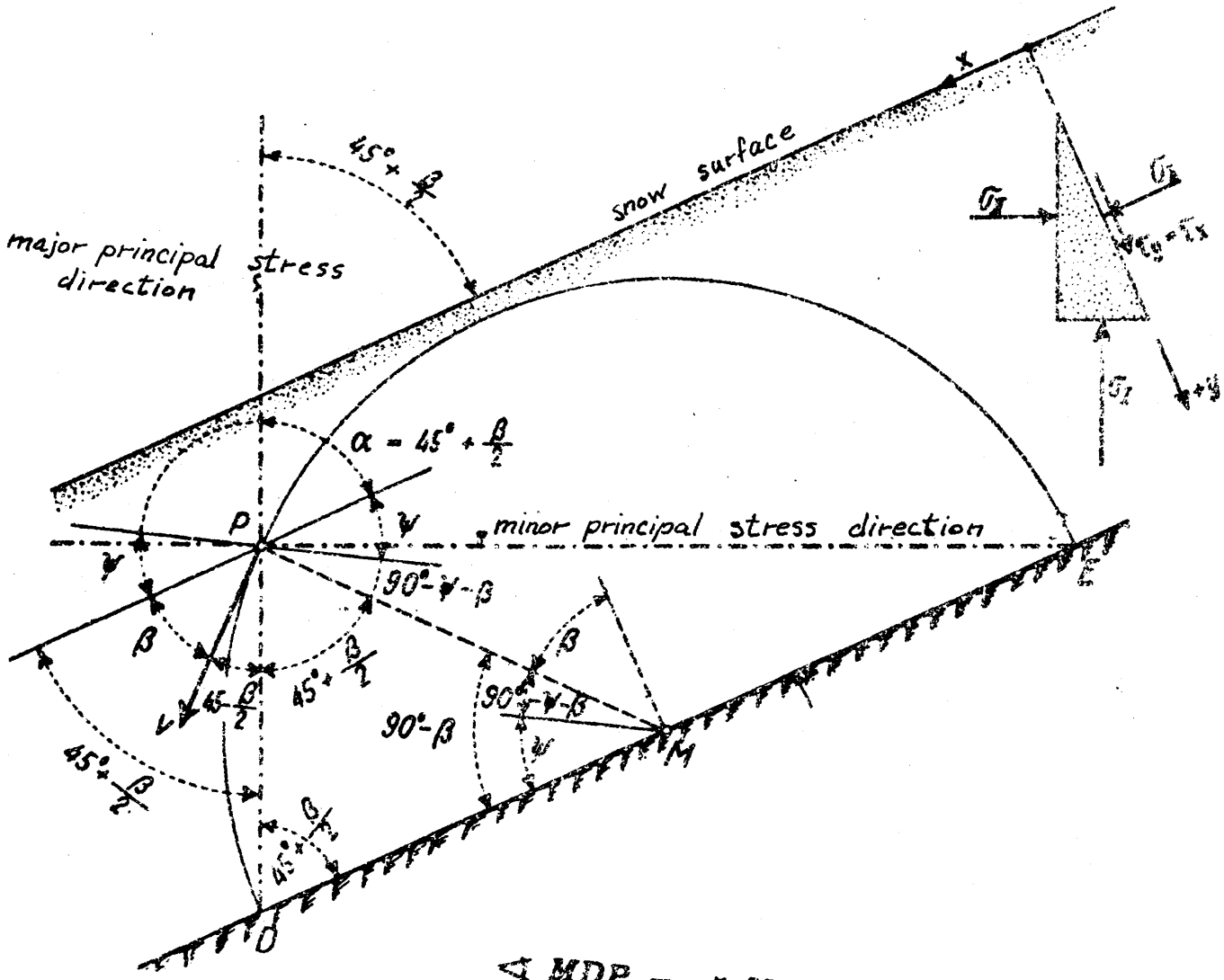

$\sphericalangle MDP = \sphericalangle MPD = \alpha$

Fig. 3 Construction of Principal Stress Direct

the stress state of the point P in the plane of the drawing, are calculated according to Fig. 3a as follows:

$$\sigma_I = \sigma_y + \tau_x \cot\alpha = y\gamma_s(\cos\psi + \sin\psi\cot\alpha)$$

$$\sigma_I = y\gamma_s[\cos\psi + \sin\psi\cot(45^\circ + \beta/2)] \quad (4)$$

$$\sigma_{II} = \sigma_y - \tau_x \tan\alpha = y\gamma_s(\cos\psi - \sin\psi\tan\alpha)$$

$$\sigma_{II} = [\cos\psi - \sin\psi\tan(45^\circ + \beta/2)] \quad (5)$$

$$\frac{\sigma_{II}}{\sigma_I} = \frac{1 - \tan\psi\tan(45^\circ + \beta/2)}{1 + \tan\psi\cot(45^\circ + \beta/2)} \quad (6)$$

From equations (4) and (5) the stress is only dependent on the creep direction β, with given values y, γ_s, ψ. Moreover, it was proven experimentally and theoretically, that during the process of metamorphosis and compression of snow, the creep angle β decreases (according to law) with an increase of bulk density. This follows from the simple consideration, that the final state of the snow layer is compressed to ice which is incompressible. This means that its deformation is only possible in one direction, which is parallel to the slope and is pure shear deformation, ($\beta = 0$). The progressive decrease of the creep angle β has a further result; the normal "setting process" of the inclined, plane, parallel, snow layer is connected with a steady change of stress configuration. This process can be called a "metamorphous stress phenomenon", which is opposite to the hydrodynamic stress phenomenon of clay becuase it is based on the metamorphosis of snow (Fig. 4a).

Such creep processes and their stress phenomena depend exclusively on the fact that the deformation of

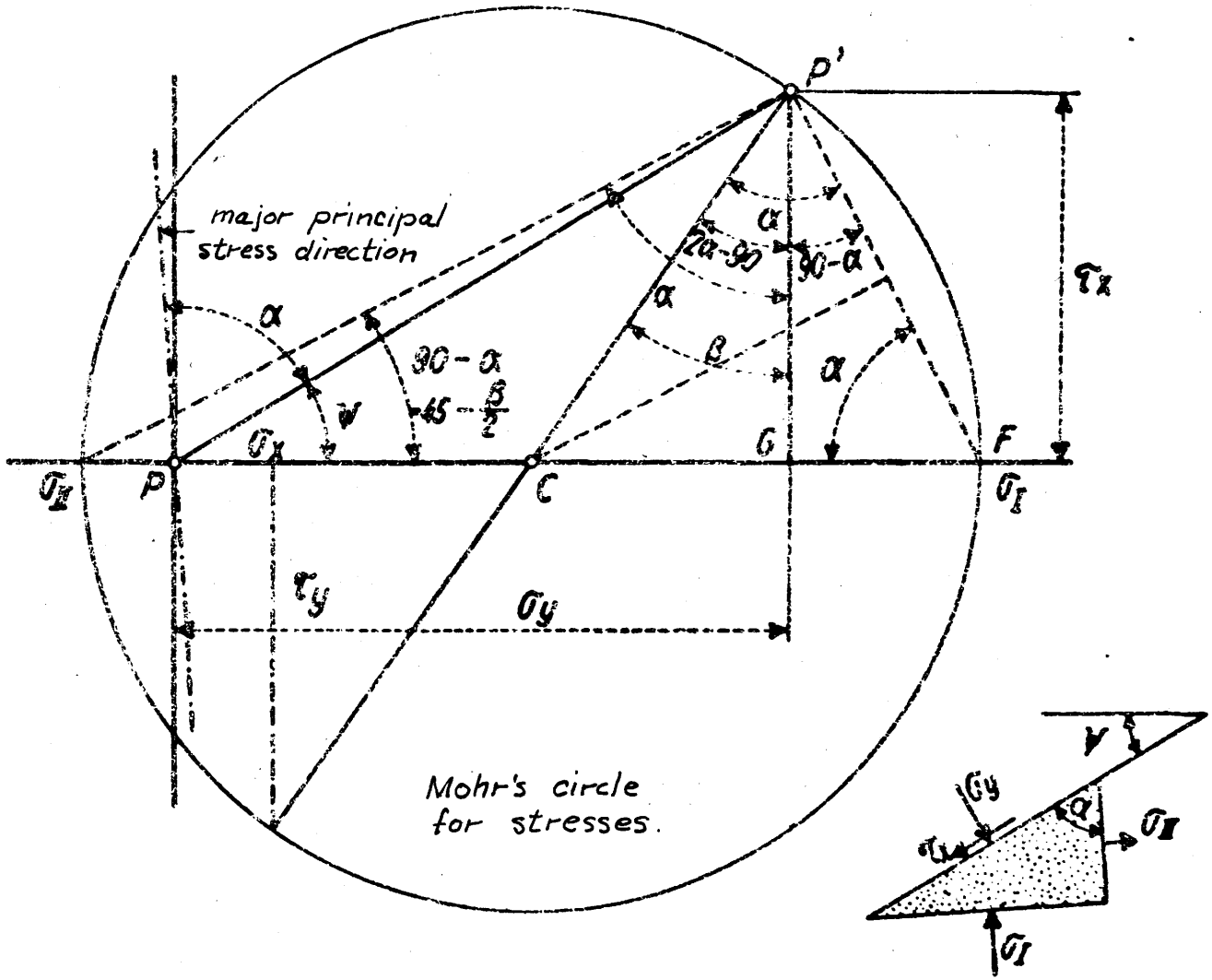

Fig. 3a Construction of Principal Stresses at a Point

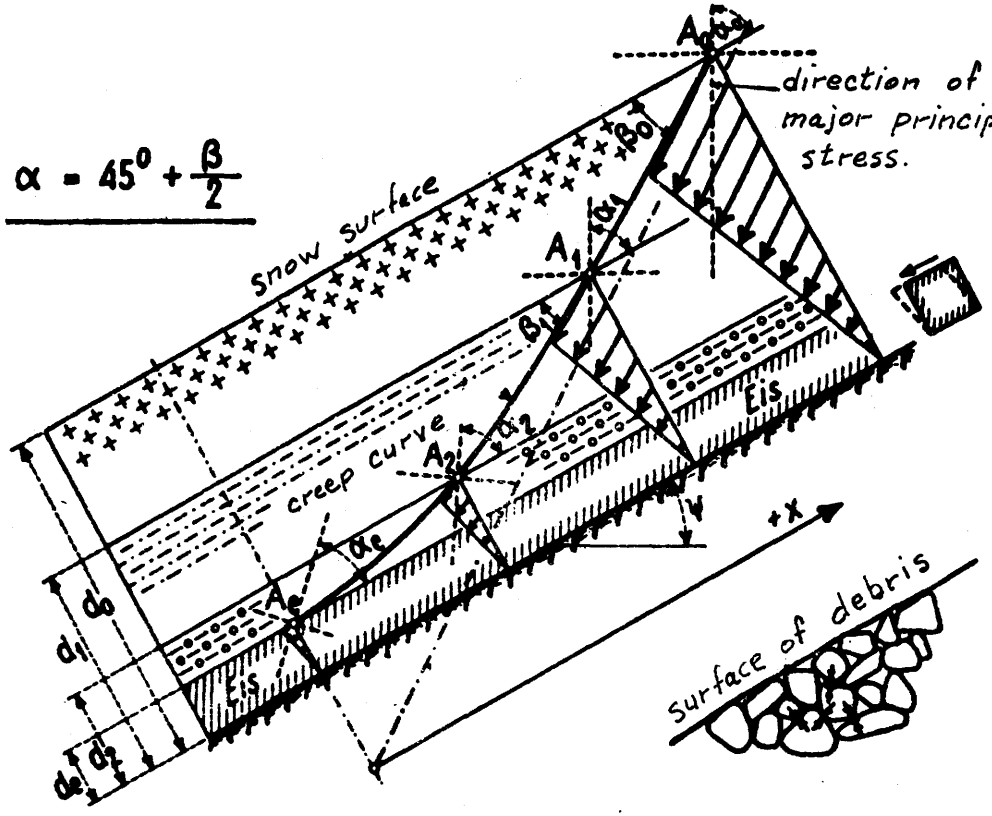

Fig. 4 Creep Process for Increasing Densities of Snow.

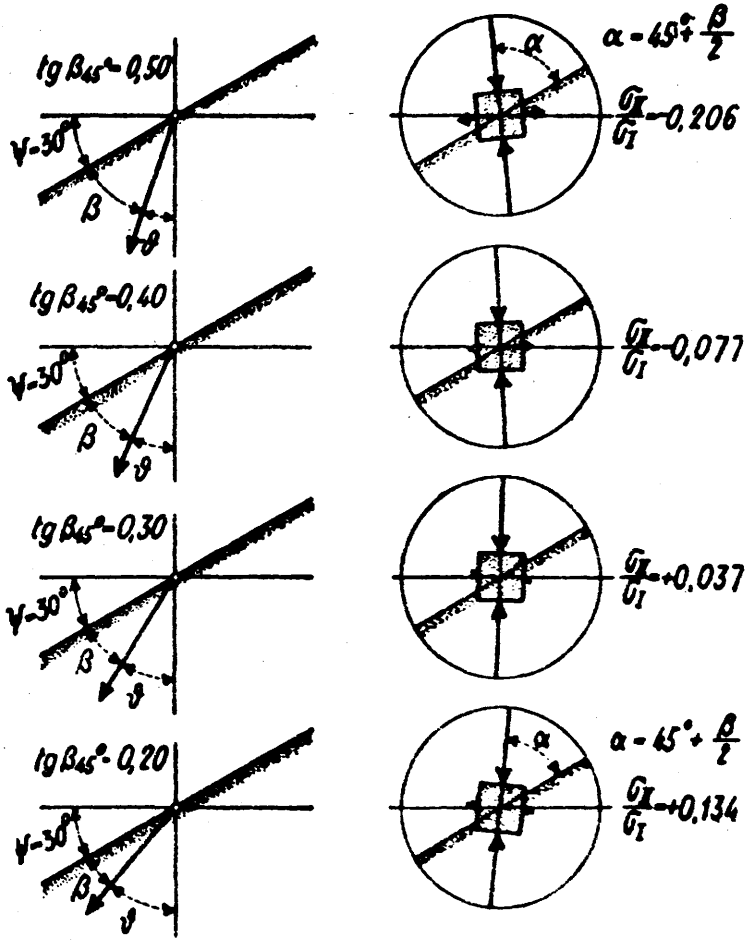

Fig. 4a Creep Directions and Principal Stresses.

single particles of the material under concern is not important. This can be observed, not only in the snow layer, but also in loose rocks. The metamorphosis of snow is, therefore, only a particular case of a general phenomenon. Strictly speaking, however, there are no particles which do not undergo some change. On a slope covered with rock and debris, which consists of mainly of coarse constituents to which water and air have free entry, the stresses which cause erosion effect a slow breaking up of the structure at the pressure transferring contact points. A compression of the grains occurs i.e. a compression of the loose mass (Fig. 4). This compression process, on the surface appears to be the same as the creep process of the sloped snow layer. The difference, however, is that it is executed much slower and can not be described by a triangular creep profile. The speed of the deformations depends mainly on the petrographic and the microclimatic conditions. In clays and loams it is mainly the intersticial water which is considered to be the root of the deformation process.

The above considerations indicate, that all slopes formed of loose rocks are in a state of slow creep movement. This movement always shows a component which is directed toward the valley. The consequences which become evident from this fact, especially in relation to the mountainous regions, are of great significance. If a building is

partly founded on compacted rock and partly on loose rock, it is exposed to a creep pressure, which is growing with time, and can lead to destruction in years to come. Statically determinate systems are in these cases superior to the statically indeterminate ones. The experiences of former years on older and recently built bridges, especially in the area of easily eroded rocks, verifies the destructive effect of the creep pressure. If slip planes are formed, the creep pressure can reach, in the limiting case, the value of the passive earth pressure. This results in the necessity of giving adequate attention to the creep movement of the subsoil, as it is a decisive factor in determining the life of the building. It should be considered also, that certain solid rocks which had grown out of soft rocks, such as clay marl, because of their reminiscent plasticity, could cause unpleasant phenomena.

To reach a generally valid method for the determination of the stress trajectories on the basis of the known deformation state, we will now try to free the described graphical method from the limitations of triangular creep profile. According to Fig. 5, we presume that the planar deformation state of the plastic body is given by the creep velocity of the point of intersection of an originally square line network. The task is now to determine the direction of the principal stresses at a nodal point of the network.

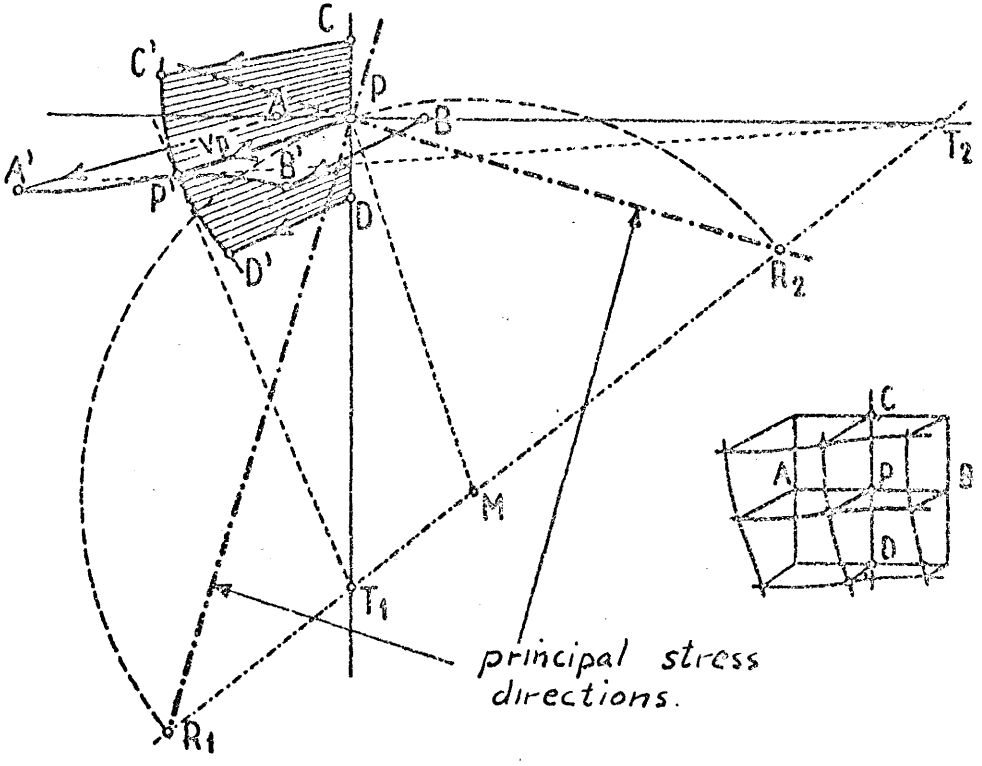

Fig. 5 General Construction for Principal Stresses

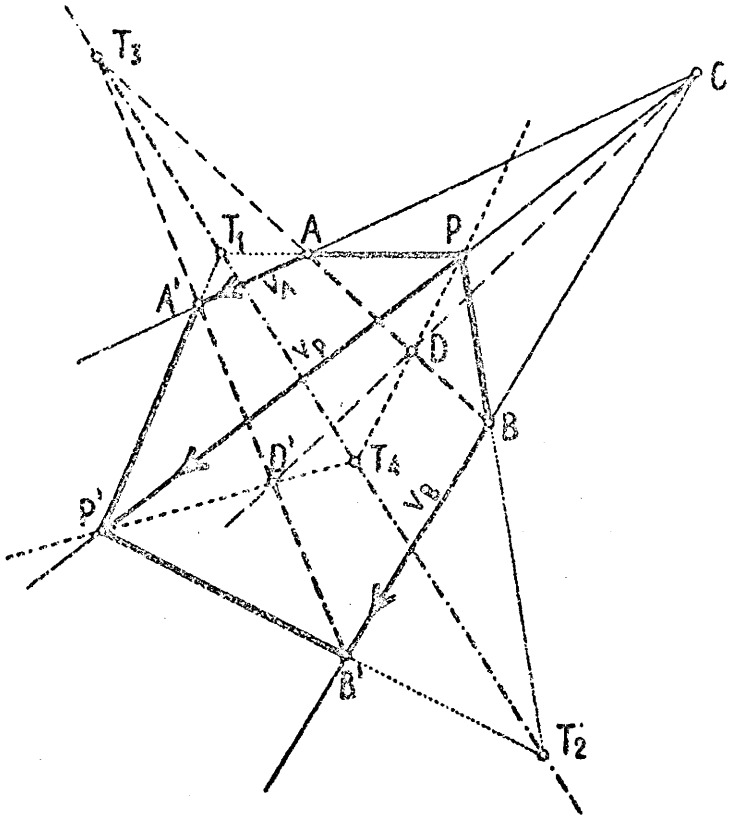

Fig. 5a Centre Collineation

The horizontal line AB changes during a unit of time, into the curve A'B', while the vertical line CD becomes the curve C'D'. The deformation state at the nodal point P and its surrounding area is given by the velocity profiles of the creep movement, which are perpendicular to each other. The horizontal profile is APB-A'P'B' and the vertical profile is CPD-C'P'D' (Fig. 5). If one draws, at the point P', the tangents to the two profile lines A'P'B' and C'P'D', they cut their respective bases at the points T_1 and T_2. The points T_1 and T_2 now appear as points of rotation for the straight lines T_1-P and T_2-P during the momentary creep movement. This results in the following relationship: the line connecting T_1 and T_2 represents the geometrical location of the instantaneous centres of all straight lines, which go through the point P on the deformed plane. The exact significance and the range of validity follows from the following example.

An indirect proof of the above statement is obtained if one assumes, that the geometric location in question is not a straight line, but any curve that runs through the points T_1 and T_2. In this case the problem of determining the principal stresses on the basis of the given values remains indeterminate i.e. there would exist an infinite number of principal stresses, which is inconceivable. The direct proof can be given generally with the help of descriptive geometry by the following method (Fig. 5a):

we draw through a point P on the deformed plane two straight lines, which go through two points, which are an infinitely small distance from each other. The three corner points, of the triangle APB, which is formed, undergo, during a unit of time, a small displacement Va, Vp, Vb so that the creep vectors intersect at the point C. The displaced corner points A'P' and B' then form a triangle which is homologous to the triangle APB, whereby, according to the theory of central projections, the "homologous" sides of this triangle intersect on a straight line T_1-T_2-T_3. If one, moreover, connects point P with a point D on the line AB and constructs the corresponding point D' on the homologous line A'B', so that the straight lines PD and P'D' also intersect a a point T_4 on the straight line T_1T_2, then the straight line T_1T_2 appears as the geometrical location of the instantaneous centres of all straight lines which go through the point P on the deformed plane. This was to be proven. The staight lines which intersect the line T_1T_2, as connecting lines of infinite adjacent points on the deformed plane, correspond to the tangents of any line drawn through P before and after defromation. This consideration is valid for very small planar deformation of a network, which moves in its own plane, so that all points travel in straight lines and at spatially regularly distributed distances. For small velocities of creep, for which the creep vectors may be

identified with the deformations which have taken place in a unit of time, the tangents, which were mentioned above, are identical to the bases of the corresponding creep profiles. The tangents to the creep profile at the original point P are the straight lines PT_1 and PT_2 and the tangents of the creep profile at the displaced point P' are $P'T_1$ and $P'T_2$ as shown in Fig. 5 and Fig. 5a.

In comparison, for large creep velocities or strongly curved creep lines, the whole consideration is only valid differentially i.e. it is to be expanded by a small time element Δt instead of a time unit. Therefore, in place of the deformations V_p , V_a and V_b , the distances $V_p \Delta t$, $V_a \Delta t$ and $V_b \Delta t$ appear. A considerable assumption further exists in that, the creep vectors of adjacent points on the deformed plane intersect at a point C of this plane, for if C moves to infinity the creep vectors may be considered as parallel. This condition which is an expression of the spatical continuity of the deformation, can normally be fulfilled.

Finally, there remains the problem of finding the two directions, which are perpendicular to each other and go through point P, and which rotate during the deformation so that the right angle between them remains unchanged. This can be done in an analogous manner as with the triangular creep profile. Erect a perpendicular on the creep velocity vector Vp at point P to intersect the straight line T_1T_2 at M.

Draw a semi-circle with radius MP and centre M to cut T_1T_2 at R_1 and R_2. The straight lines R_1P and R_2P represent the sought after directions of the principal stresses. Since the right angle which is formed between these two directions stays constant with a small change of point P in the direction Vp, and since this is only possible with a plastic material when in these directions only small shearing stresses are effective, then the direction of the principal stresses has been proven. The solution given for the triangular creep profile appears now as a special case (Fig. 3).

The above method can be used for the experimental investigation of plastic deformations occuring in the planar stress state. Consider for instance, the model of a retaining wall (Fig. 6), filled with a plastic material. Under the side pressure of this material, the wall suffers a certain measureable deformation. The deformations of an originally square line network were measured similarly to that in the snow laboratory (Fig. 7). The distribution of side pressure on the wall AD is required. The known creep profile allows, first of all, the determinations of the principal stress directions, where by the course of the trajectories could be given and recorded (drawn). If one sets the side pressure of the wall BC as known, (by a graphic method of the force composition and analysis) the approximate distribution of the side pressures and

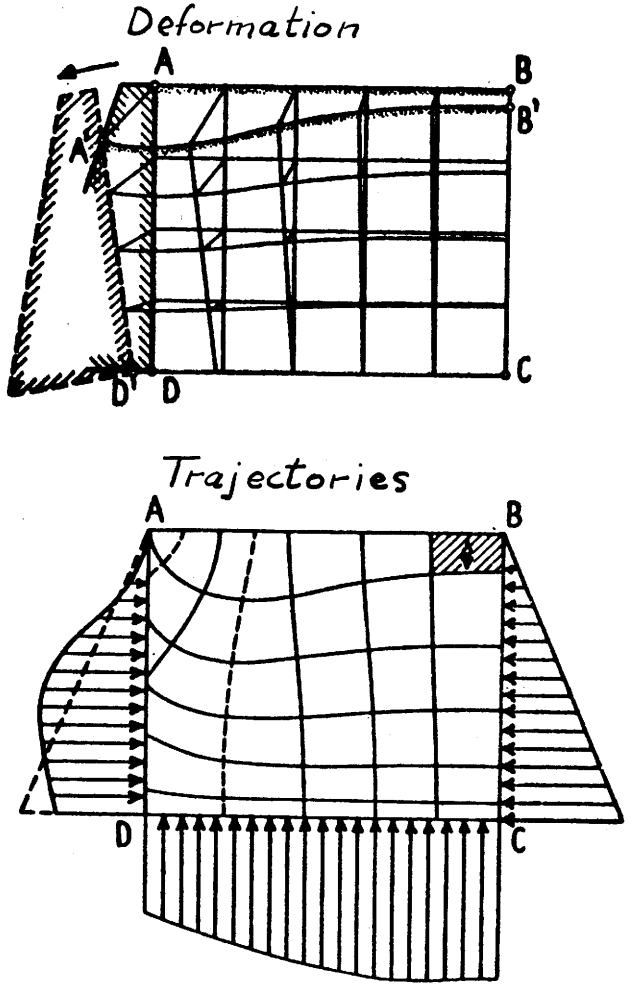

Fig. 6 Example of the Determination of Stress Trajectories.

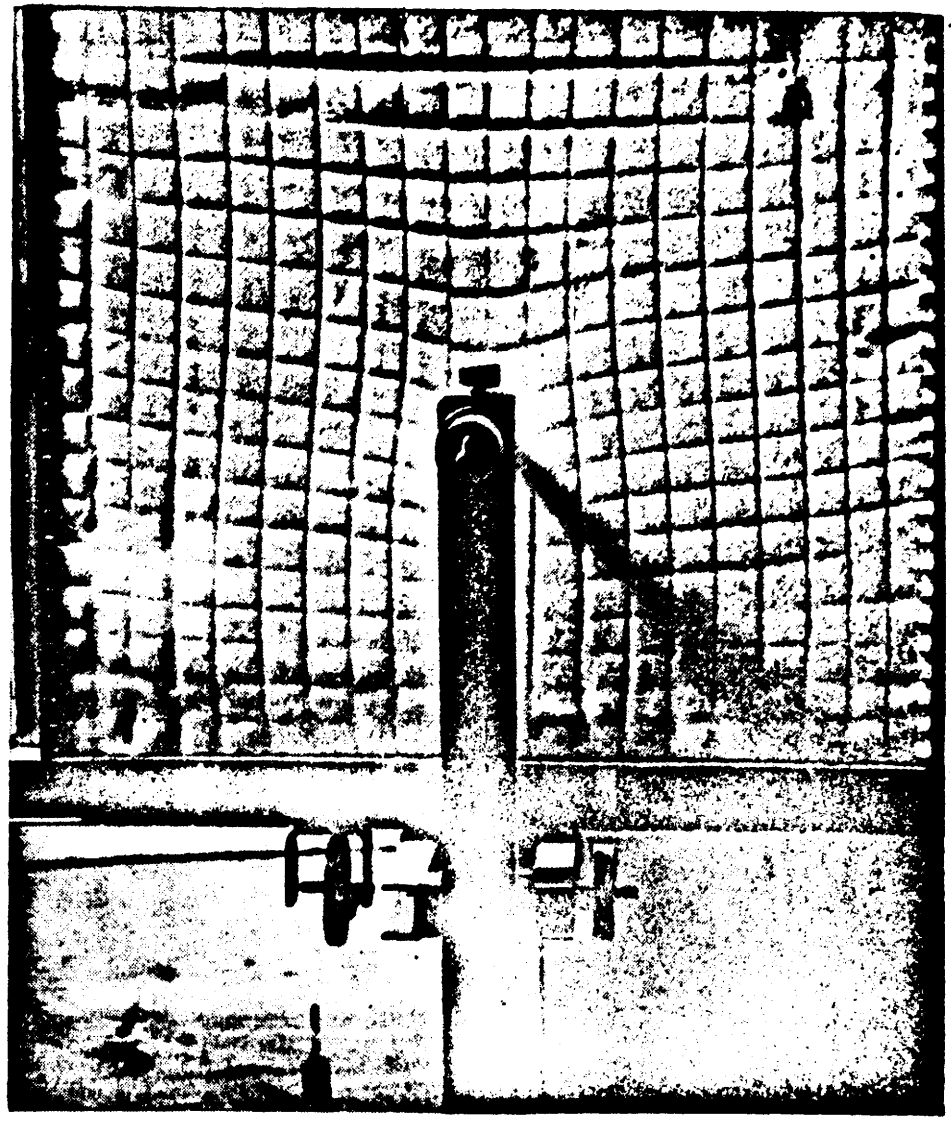

Fig. 7 Deformation of an Originally Square Line Network.

friction forces as well as the pressures on the base C-D can be determined. Depending on the movement of the supporting wall, a more or less large discrepancy will exist between the force distribution of the side pressures and the triangular distribution of the classical earth pressure theory. With that, a method is indicated which under certain circumstances offers considerable facilities for the clarification of planar stress states in plastic bodies, by the determination of the principal stress directions. This method is valid not only for plastic deformation, but also for elastic deformation.

TABLE I

TABLE I

Measured and Corrected Co-ordinates for Seven Markers

Marker No.	Wheel Location (inches)	Measured Co-ordinates (inches)		Corrected Co-ordinates (inches)		Depth to Original Marker Position (inches)
		X	Y	X	Y	
1.		-3.78	3.32	-3.240	2.845	3.035
	11.8R	-3.82	3.38	-3.274	2.897	
	6.0R	3.91	3.42	-3.354	2.931	
	0	-4.17	3.08	-3.574	2.640	
	6.0L	-3.52	3.13	-3.017	2.682	
	11.6L	-3.59	3.28	-3.077	2.811	
	16.6L	-3.61	3.27	-3.094	2.802	

Correction Factor = 0.857

TABLE Ia

Measured and Corrected Co-ordinates for Seven Markers

Marker No.	Wheel Location (inches)	Measured Co-ordinates (inches)		Corrected Co-ordinates (inches)		Depth to Original Marker Position (inches)
		X	Y	X	Y	
2.		-2.57	3.21	-2.202	2.751	3.129
	11.8R	-2.63	3.28	-2.254	2.811	
	6.0R	-2.74	3.33	-2.348	2.854	
	0	-2.91	2.74	-2.494	2.348	
	6.0L	-2.37	3.13	-2.031	2.682	
	11.6L	-2.42	3.18	-2.074	2.725	
	16.6L	-2.44	3.17	-2.091	2.717	

Correction Factor = 0.857

TABLE Ib

Measured and Corrected Co-ordinates for Seven Markers

Marker No.	Wheel Location (inches)	Measured Co-ordinates (inches)		Corrected Co-ordinates (inches)		Depth to Original Marker Position (inches)
		X	Y	X	Y	
3.		-1.32	3.37	-1.131	2.888	2.922
	11.8R	-1.40	3.45	-1.200	2.957	
	6.0R	-1.52	3.49	-1.302	2.991	
	0	-1.47	2.75	-1.260	2.357	
	6.0L	-1.09	3.29	-0.934	2.820	
	11.6L	-1.13	3.28	-0.968	2.811	
	16.6L	-1.15	3.29	-0.986	2.820	

Correction Factor = 0.857

TABLE Ic

Measured and Corrected Co-ordinates for Seven Markers

Marker No.	Wheel Location (inches)	Measured Co-ordinates (inches)		Corrected Co-ordinates (inches)		Depth to Original Marker Position (inches)
		X	Y	X	Y	
4.		-0.08	3.28	-0.069	2.811	3.069
	11.8R	-0.17	3.39	-0.146	2.905	
	6.0R	-0.33	3.40	-0.283	2.914	
	0	-0.03	2.61	-0.026	2.237	
	6.0L	0.09	3.19	0.077	2.734	
	11.6L	0.05	3.17	0.043	2.717	
	16.6L	0.04	3.17	0.034	2.717	

Correction Factor = 0.857

TABLE Id

Measured and Corrected Co-ordinates for Seven Markers

Marker No.	Wheel Location (inches)	Measured Co-ordinates (inches)		Corrected Co-ordinates (inches)		Depth to Original Marker Position (inches)
		X	Y	X	Y	
5.		1.21	3.37	1.037	2.888	2.992
	11.8R	1.10	3.48	0.942	2.982	
	6.0R	0.89	3.42	0.762	2.931	
	0	1.37	2.79	1.174	2.391	
	6.0L	1.36	3.26	1.166	2.794	
	11.6L	1.32	3.23	1.131	2.768	
	16.6L	1.32	3.22	1.131	2.760	

Correction Factor = 0.857

TABLE Ie

Measured and Corrected Co-ordinates for Seven Markers

Marker No.	Wheel Location (inches)	Measured Co-ordinates (inches)		Corrected Co-ordinates (inches)		Depth to Original Marker Position (inches)
		X	Y	X	Y	
6.		2.39	3.37	2.048	2.888	2.992
	11.8R	2.27	3.50	1.945	3.000	
	6.0R	2.01	3.29	1.722	2.820	
	0	2.62	2.95	2.245	2.528	
	6.0L	2.53	3.28	2.168	2.811	
	11.6L	2.50	3.23	2.142	2.768	
	16.6L	2.49	3.23	2.134	2.768	

Correction Factor = 0.857

TABLE If

Measured and Corrected Co-ordinates for Seven Markers

Marker No.	Wheel Location (inches)	Measured Co-ordinates (inches)		Corrected Co-ordinates (inches)		Depth to Original Marker Position (inches)
		X	Y	X	Y	
7.		3.58	3.32	3.068	2.845	3.035
	11.8R	3.42	3.46	2.931	2.965	
	6.0R	3.16	3.02	2.708	2.588	
	0	3.79	3.06	3.248	2.622	
	6.0L	3.70	3.21	3.171	2.751	
	11.6L	3.66	3.19	3.137	2.734	
	16.6L	3.67	3.19	3.145	2.734	

Correction Factor = 0.857